MORC2 restriction factor silences HIV proviral expression

Angélique Lasserre[1], Sébastien Marie[1,#], Marina Morel[1,#], Michael M. Martin[1], Alexandre Legrand[2], Virginie Vauthier[1], Andrea Cimarelli[2], Lucie Etienne[2,] Florence Margottin-Goguet[1], Roy Matkovic[1,*]*

[1]Institut Cochin, Université Paris Cité, INSERM U1016, CNRS UMR8104, Paris, France
[2]CIRI, Centre International de Recherche en Infectiologie, Inserm U1111, Université Claude Bernard Lyon 1, CNRS UMR5308, Ecole Normale Supérieure de Lyon, Univ Lyon, Lyon, France

[#]equal contribution
**corresponding authors*
Contact: roy.matkovic@inserm.fr ; lucie.etienne@ens-lyon.fr

Abstract (250 words max)

The HUSH complex (composed of TASOR, MPP8 and periphilin) represses HIV-1 expression from its promoter by inducing both propagation of repressive epigenetic marks and degradation of the nascent transcript. Vpx from HIV-2, and Vpr proteins from some simian lentiviruses (SIVs), antagonize HUSH, thereby increasing proviral expression. The chromatin-remodelling MORC2 protein plays a critical role in the epigenetic silencing of host genes by HUSH. Here, we deciphered the role of MORC2 in retroviral silencing. We show that MORC2, in contrast to HUSH components, presents strong signatures of positive selection during primate evolution. Like HUSH, MORC2 represses proviral expression in two models of HIV-1 latency. However, while HUSH is degraded upon HIV-2 infection in a Vpx-dependent manner, MORC2 levels are increased, raising the question of a feedback control mechanism without HUSH. Upon infection with an HIV-1-derived virus, MORC2 and TASOR antiviral effects are interdependent. However, once the lentiviral DNA is integrated into the host genome, MORC2 may maintain the repression independently of HUSH. At the post-transcriptional level, both MORC2 and HUSH act in association with CNOT1 of the CCR4-NOT deadenylase complex and the TRAMP-like PAXT complex. Finally, MORC2, but not HUSH components, is expressed in primary quiescent CD4+ T cells. Altogether, our data highlight MORC2 as an HIV restriction factor and a chromatin remodelling protein operating both at the transcriptional and post-transcriptional levels. We speculate that MORC2 could serve as an immune gatekeeper following HUSH inactivation by Vpx and contribute to the maintenance of retroviral silencing in reservoir CD4+ T cells.

Significance statement (120 words max)

One hurdle to HIV eradication is viral latency, which refers to the persistence of the virus in reservoir cells despite antiretroviral treatment. The HUSH complex represses HIV expression, once the viral

genome is integrated into the host genome. HUSH activity on host genes depends on MORC2, a protein incriminated in the Charcot-Marie-Tooth neuronal disease. Here, we first show that MORC2 presents signs of evolutionary arms-races in primates. Furthermore, MORC2 contributes to HIV silencing in cooperation with HUSH, but also, likely without HUSH. Despite identified as a chromatin remodeler, MORC2 also works at a post-transcriptional level. Altogether, MORC2 appears as a host defense factor, which plays a role in HIV latency.

Introduction

Human Immunodeficiency viruses type 1 and 2 (HIV-1 and 2) are responsible for Acquired Immunodeficiency Syndrome (AIDS). Their eradication faces a major obstacle that is viral persistence in reservoir cells, despite antiretroviral treatment. HIV latency refers to silent viruses, which can produce infectious particles in case the treatment is interrupted. While HIV has long been thought to be transcriptionally inactive in latently infected cells, more and more evidence now show that transcription can occur in these cells and that latency operates at several levels, including post-transcriptional levels. Proviral transcriptional activity is associated with activating epigenetic chromatin features in proximity of integration sites in infected individuals(1).

Among several host proteins involved in the repression of the HIV-1 provirus integrated into the host genome, the human silencing hub (HUSH) complex, formed by transcription activation suppressor (TASOR), M-phase phosphoprotein 8 (MPP8) and periphilin has recently emerged as a critical component. On one hand, HUSH represses HIV and lentiviral expression, while on the other hand, HUSH is counteracted by lentiviral proteins, including Vpx from HIV-2 and Vpr from several non-human primate lentiviruses(2-4). From an evolutionary standpoint, viral antagonism of the host antiviral factors, the so-called host restriction factors, often triggers a strong pressure on the host protein, and only proteins able to escape antagonism will be selected along evolution. In turn, the viral protein is also submitted to adaptation cycles. This molecular arms-race between viral proteins and host proteins can notably be witnessed by the presence of sites under positive selection, particularly at the direct virus-host molecular interface(5-7). Over million years of coevolution, these marks result from the selection of advantageous mutations in the host (an excess rate of non-synonymous substitutions (dN) compared to the rate of synonymous substitutions (dS)) and can be witnessed by analysing protein-coding sequences of orthologous genes (i.e. from different host species). Such signatures of positive selection are for example present in the HIV restriction factors SAMHD1, APOBEC3G or Tetherin/BST-2 –all three antagonized by specific lentiviral proteins (reviewed in(6)). Despite HUSH being degraded by lentiviral lineage-specific proteins, HUSH subunits are not characterized by strong positively selected sites, but rather by other potential diversification through multiple isoforms(2).

The mechanism by which HUSH recognizes and silences HIV is still poorly understood. It relies on the activity of several interconnected protein complexes. Through its chromodomain, MPP8 binds H3K9me3 marks, driving HUSH to its genomic loci and, in turn, mediating the recruitment of the SETDB1 methyltransferase(8). This result in the writing of additional H3K9me3 marks and the spreading of heterochromatin on an exogenous transgene in a position-effect variegation process, meaning silencing might happen only in an adequate repressive environment(8). But HUSH also works at the post-

transcriptional level. Our group highlighted a cooperation between TASOR and CNOT1 that synergistically destabilize nascent transcripts synthesized from the HIV-1 LTR promoter(9). Cooperation between HUSH and the RNA decay machinery was also shown to operate on host transposable elements in mouse ESC lines(10).

Following the discovery of HUSH, MORC2 (Microrchidia family CW-type zing finger 2) was identified as a protein critical for HUSH-mediated epigenetic silencing of host genes(11). Alterations in the MORC2 gene are associated with the Charcot Marie Tooth disease(12-16). MORC2 belongs to the MORC ATPase superfamily (MORC1-4 and the divergent SMCHD1), which has been implicated in epigenetic silencing in diverse organisms(17-19). It is a chromatin-remodelling protein, which contains, alike other proteins from the family, an N-terminal gyrase, Hsp90, histidine kinase and MutL (GHKL)-type ATPase domain and a CW-type zinc finger histone recognition module(17). In addition, MORC2 possesses a C-terminal chromo-like domain (CD domain), which is a domain involved in the recognition of methylated peptides in histones and non-histone proteins, though the function of this domain in MORC2 has not been elucidated(17). MORC2 is also involved in the DNA damage response contributing to a PARP-1-dependent repair pathway(20) and in the cell cycle control through an acetylation-dependent mechanism(21). Regarding HUSH, the HUSH complex recruits MORC2 to specific loci, where the MORC2 ATPase and CW domains are required for HUSH silencing(11). In contrast, the CD domain does not appear important for MORC2 repression activity(11). Because chromatin remodelling *in vitro* relies on the ATPase activity(22), the group of Lehner proposed that MORC2 remodelling activity is required to alter chromatin architecture and to promote gene silencing by HUSH(11). Indeed, loss of MORC2 results in the loss of H3K9me3 marks, chromatin decompaction and loss of transcriptional silencing at HUSH target sites(11). Apart its broad distribution across H3K9me3-marked heterochromatin, MORC2 was also visualized at transcription start sites (TSSs) independently from HUSH, the functional relevance of this TSSs localization is unknown(11).

Whether MORC2 is involved in the silencing of the HIV-1 provirus has not been investigated yet. We show here that MORC2 presents the features of a restriction factor with strong signatures of positive selection as well as antiviral activity. We also provide lines of evidence suggesting that MORC2 could operate independently from HUSH in the maintenance of retroviral silencing. Because only MORC2, as opposed to HUSH components, is detected in primary CD4+ quiescent T cells, we speculate that MORC2 is a key player for the silencing of HIV in reservoir cells of infected individuals.

Results

The presence of strong signatures of positive selection during primate evolution is a frequent characteristic of lentiviral restriction factors(6). When MORC2 was identified as a protein essential for HUSH repression, we wondered whether MORC2 has been evolving under positive selection in primates, in contrast to HUSH components(2). To address this possibility, we analysed MORC2 orthologous sequences from 25 species of primates, reconstructing its evolutionary history on 60-80 million years of divergence. The topology of the phylogenetic tree reconstructed from the primate MORC2 coding sequences was concordant with the primate species tree (Fig. 1A). To determine if MORC2 has evolved under positive selection, we performed several positive selection analyses

available in the Detection of Genetic INNovation (DGINN) pipeline and from the HYPHY package (see Methods)(23). We first found strong evidence of positive selection at the gene-wide level in primate MORC2 (Fig. 1B). Furthermore, site-specific analyses identified at least nine sites undergoing rapid evolution, notably in the C-terminal part of the protein (Fig. 1C-D). The presence of two clusters of positively selected residues in the disordered regions surrounding the chromo-like domain (CD) may indicate viral specificity domains(24) (Fig. 1E-F). These results show that MORC2 has been involved in a molecular conflict along evolution and suggest that it could play a unique role in HUSH-mediated HIV restriction.

We therefore investigated whether MORC2 restricts an HIV-1-derived virus. HeLa cells were infected with a HIV-1-LTR-CMV virus, pseudo-typed with the G envelope protein of the Vesicular Stomatitis Virus (VSV) virus. This virus, previously identified as a good readout of HUSH activity(2), drives the expression of luciferase (luc) from the CMV promoter, once the reverse transcribed DNA has been integrated into the host genome, thanks to the two HIV-1 Long Terminal Repeats (LTR). We found that MORC2 depletion increased luc expression, while the overexpression of wt MORC2, decreased luc expression (Fig. 1G, left and 1H). The ATPase-defective MORC2 mutant (D68A), required for chromatin remodelling and HUSH activity(11, 22), lost this capacity, suggesting a post-integration effect on viral expression (Fig. 1H). Restriction was also obtained with a SIVmac-derived virus, suggesting MORC2 has a broad anti-lentiviral activity (Fig. 1G, right). We further addressed the possibility that MORC2 primate orthologs could have different abilities to repress HIV-1, as species-specificity may emerge from rapidly evolving restriction factors. Testing four MORC2 orthologous proteins from highly divergent primate species, we found that they similarly repressed viral expression (Fig. 1H). These results show that MORC2 detains a well conserved autonomous repressive activity. Furthermore, because our heterologous virus-host assay (from four primate species MORC2) sampled diverse amino acids at the positively selected sites (Fig. 1D), this suggests that positive selection of MORC2 is not linked to the restrictive effector function against the HIV-1-derived virus. Together, our results suggest that primate MORC2s detain a well conserved autonomous repressive activity of lentiviruses.

Given that HUSH recruits MORC2 and is inactivated by divergent lentiviral Vpr or Vpx proteins and that both HIV-2/SIVsmm Vpx and HIV-1 Vpr were reported to enhance LTR-driven transcription(2, 25-28), we investigated whether HIV-2/SIVsmm Vpx or HIV-1 Vpr could antagonize MORC2 or use MORC2 for their functions. In contrast to HUSH, MORC2 was not degraded following infection by a complete wt HIV-2 virus and, instead, was stabilized (Fig. 2A). This effect was lost with the virus deleted of Vpx or of Vpr and Vpx, but not with the ΔVpr virus, pointing out to an effect of Vpx (Fig. 2A). Accordingly, Vpx-containing Viral-Like pseudo-Particles (VLPs) induced TASOR degradation and MORC2 stabilization as reported in(4) (Fig. 2B). Because MORC2 mRNA levels were enhanced by HUSH depletion(11) and Sup. Fig. 1A), this stabilization likely results from a transcriptional effect. Regarding HIV-1, MORC2 levels were not impacted by HIV-1 infection, while levels of the HLTF DNA translocase were slightly reduced in a Vpr-dependent manner (Sup. Fig. 1B). Of note, none of the proteins from a group of divergent lentiviral Vpr and Vpx proteins could induce MORC2 destabilization (Sup. Fig. 1C).

We further wondered whether MORC2 could serve as a bridge between HUSH and Vpx in order to induce HUSH degradation. This is not the case since MORC2 depletion did not impair Vpx-mediated

HUSH degradation (Fig. 2C, compare 3,4 to 1,2). Similarly, the depletion of MORC2 did not impact Vpr-mediated HLTF degradation (Sup. Fig. 1D, compare lanes 4,5 to 1,2), in contrast to the depletion of DCAF1, the ubiquitin ligase adaptor used by Vpr to degrade HLTF (Sup. Fig. 1D, lane 6)(29, 30). Altogether, these results suggest that HIV-2 Vpx and HIV-1 Vpr do not induce MORC2 degradation, nor do they use MORC2 to induce the degradation of HUSH or HLTF, respectively. Nonetheless, they do not rule out the possibility that Vpx or Vpr could inactivate MORC2 in any way other than degradation. To address this issue, we further reasoned that prior treatment with a given viral protein would inhibit the subsequent effect of MORC2 depletion, if MORC2 was inactivated by the viral protein. Hela cells were first infected by the HIV-1-LTR-CMV-luciferase virus, then, 2 days later, treated with Vpx or Vpr-containing VLPs, then, the following day, treated with siRNA directed against MORC2. The depletion of MORC2 still enhanced luciferase expression whether cells were pre-treated or not with Vpx or Vpr-containing VLPs, suggesting that the two viral proteins did not efficiently antagonize MORC2 (Fig. 2D, Sup. Fig. 1E). This result also suggests that MORC2 may maintain the repression independently from TASOR, which has been depleted by Vpx prior to MORC2 siRNA treatment, though a tiny amount of TASOR left after Vpx delivery might be sufficient for MORC2 activity. In contrast, when TASOR was depleted prior infection by the virus (HeLa cells Crispr/Cas9 for TASOR), MORC2 siRNA had no further effect, and conversely (Fig. 2E), suggesting that TASOR and MORC2 rely on each other upon infection to silence an incoming virus. Finally, depletion of MORC2 in HeLa cells did not increase viral expression following infection by a single cycle ΔEnv HIV-2 virus, whose Nef gene was replaced by luciferase, in the presence or the absence of Vpx, suggesting again that Vpx does not antagonize MORC2 (Sup. Fig. 2).

To further investigate the mechanism of MORC2 restriction, we used a cellular system in which LTR-driven transcription could be studied independently of RNA splicing and RNA polymerase II (RNAPII) pausing(9). In this system, Hela cells harbor one unique and monoclonal copy of an integrated LTR-luciferase construct with a deleted TAR sequence that blocks RNAPII elongation, allowing productive transcription. By chromatin-immunoprecipitation, we found that MORC2 is able to bind the HIV promoter (Fig. 3A). Interestingly, no signal was seen on the coding sequence (here luciferase) despite HUSH being detected both on promoters and coding sequences(31). Because HUSH contributes to the degradation of nascent transcripts, we also wondered whether MORC2 could operate at the post-transcriptional level. Thus, we performed a *Nuclear Run On* experiment to distinguish MORC2 effects on nascent luciferase transcript levels, labelled with BrUTP, and on total luciferase mRNA levels. As expected, TASOR down-regulation poorly impacted the levels of nascent transcripts in this system, while it triggered a 2.3-fold increase of steady-state Luc RNA levels, in agreement with TASOR involved in the turnover of LTR-driven transcripts (Fig. 3B)(9). For its part, MORC2 depletion impacted both nascent transcript (1.8 fold) and, to a greater extent, total transcript (3.8 fold) levels, suggesting an effect of MORC2 both at the transcriptional and post-transcriptional levels (Fig. 3B). In addition, the silencing of both MORC2 and CNOT1 expression induced a strong synergistic effect, of the same range as the one induced by TASOR and CNOT1 depletion (Fig. 3C)(9). The triple depletion of TASOR, MORC2 and CNOT1 resulted in the additive effect of the depletion of MORC2-CNOT1 on the one hand and MORC2-TASOR on the other hand, suggesting that MORC2 might operate with CNOT1 independently from

TASOR (Fig. 3C). In line with a MORC2-CNOT1 cooperation, we retrieved endogenous MORC2 in a CNOT1 immunoprecipitate and CNOT1 in a MORC2 immunoprecipitate, highlighting an interaction between the two proteins (Fig. 3D). This interaction was reduced by RNAse A treatment, suggesting that RNA favors the association between MORC2 and CNOT1 (Fig. 3D). Furthermore, the interaction was still detected in cells depleted of TASOR, while the CNOT1-TASOR interaction was detected in cells depleted of MORC2, again suggesting that MORC2 could operate independently from TASOR (Sup. Fig. 3A). To further highlight the connection of MORC2 with the RNA metabolism pathway, we questioned whether MORC2, alike TASOR, could interact with the MTR4 RNA helicase and Zinc finger ZFC3H1-type containing protein (ZFC3H1)(9). In yeast, MTR4 interacts with the yeast homolog of CNOT1, resulting in the degradation of nascent RNAs(32, 33). In humans, MTR4 is present in different complexes that use the exosome for the degradation of a target RNA, in particular the TRAMP-like PAXT complex that contains the ZFC3H1 subunit(34, 35). In an exogenously expressed MORC2 immunoprecipitate, we retrieved CNOT1, but also MTR4 and ZFC3H1 (Fig. 3E). Despite CNOT1 interacts with CD domain-containing proteins such as MPP8(36), the removal of MORC2 CD domain did not impact its interaction with CNOT1, MTR4 and ZFC3H1 (Fig. 3E). In addition, endogenous TASOR and endogenous MORC2 both interact with CNOT1 (Sup. Fig. 3B). Altogether, MORC2 appears to operate not only at the transcriptional level, but also at the post-transcriptional level, in cooperation with RNA degradation proteins.

Next, we questioned the role of MORC2 in more relevant cell models of HIV infection. First, we found that TASOR and MORC2 were both expressed in activated primary CD4+ T cells at the protein level, but only MORC2 could be detected in non-activated CD4+ T cells (Fig. 4A). Then, we used the J-Lat A1 HIV-1 model of latency, derived from the Jurkat T cell line, which contains an HIV-1 LTR-*tat*-*IRES*-*gfp*-LTR minigenome stably integrated at a unique site and epigenetically silenced(37). An increase in the percentage of GFP-positive cells is indicative of viral reactivation from the latent state. The depletion of MORC2 by Crispr/Cas9 led to an increase of the percentage of GFP-positive cells (Fig. 4B). Cells were FACS-sorted according to GFP expression (no, low or high GFP expression) and put back in culture for two weeks. Western blot analyses confirmed that the more MORC2 was depleted, the more GFP was expressed (Fig. 4B, western blot right). Secondly, we used another model of HIV-1 latency, in which Jurkat T cells were first infected with an HIV-1 virus that retains complete LTRs, Tat and Rev, but has a frameshift mutation in Env, nef growth factor receptor (ngfr) in place of Nef and GFP in place of Gag, Pol, Vif and Vpr(4). In this case, infected cells represent a population with diverse integration sites. EGFP-positive cells were sorted by cytometry, kept in culture until EGFP expression was silenced, and finally EGFP-negative cells were sorted to get a latency model as described in(4, 9). Depletion of MORC2 led to a 2-fold increase of the percentage of GFP-positive cells, without or with the TNFα transcriptional inducer (Fig. 4C). Altogether, MORC2 appears as a player in the silencing of HIV-1 in two models of latency.

Discussion

MORC2 harbors signatures of positive selection along primate evolution, one of the well-defined characteristics of antiviral restriction factors. On one hand, MORC2 could be considered as a component

of the previously described HUSH complex, which is destabilized in the presence of divergent Vpx and Vpr proteins. Indeed, HUSH and MORC2 interact, and both proteins rely on each other for the silencing of incoming viruses, as shown here, or for the silencing of host genes(11). Therefore, HUSH associated with MORC2 could be envisioned as a single multi-subunit restriction factor that could provide different interfaces for viral attacks. In the case of the SAMHD1 restriction factor, Vpx/Vpr proteins from divergent viruses, despite their common origin and structural homology, target entirely different domains of the host protein in a species-specific manner(38-40). This difference in SAMHD1 recognition is evolutionarily dynamic and is further witnessed by sites of positive selection in both N- and C- terminal domains of the host protein(38, 41, 42). Analogously, we initially hypothesized that HUSH-MORC2 could be targeted by different ways through their different subunits: HUSH targeted by Vpx and MORC2 potentially by another lentiviral protein of the Vpr/Vpx family, which could have explained the presence of a positive selection signature in MORC2. These positively selected residues form two clusters in the disordered regions, which are also known to be frequent targets of positive selection(43, 44). These regions could constitute interfaces for binding and coupled folding with other proteins such as the HUSH complex, or viral proteins, where the subsequent acquired structure could vary depending on the partners. Furthermore, it should be noted that the AlphaFold structure prediction score of MORC2 is low for these regions (Sup. Fig. 4), which is the case for most disordered proteins. The positive role of HIV-1 Vpr and HIV-2/SIVsmm Vpx on proviral expression, made these proteins prime candidates among proteins susceptible to inactivate MORC2. Theoretically, several scenarios would have been possible: two different proteins of the same lentiviral lineage, or two proteins from different lineages, or the same viral protein could target HUSH and MORC2. In any event, infection by HIV-1 or HIV-2 viruses does not downregulate MORC2 expression, suggesting that MORC2 is not degraded by any of the viral proteins encoded by these viruses. We were also unable to detect any downregulation of MORC2 in the presence of a set of lentiviral Vpr and Vpx proteins from different origins. Obviously, it must be kept in mind that inactivation of a host restriction factor by a viral protein may result from a mechanism other than degradation(45, 46). Prior delivery of HIV-1 Vpr or HIV-2/SIVsmm Vpx to cells does not prevent the effect of the subsequent depletion of MORC2, suggesting that these viral proteins do not inactivate MORC2 in any way. We also wondered whether MORC2 could be a direct adaptor recruited by Vpx or Vpr to induce the degradation of their targets, such as CBFβ is recruited by Vif to ensure APOBEC3G degradation(47, 48). Though, noteworthy, CBFβ is evolutionary and structurally well conserved with no obvious sites of positive selection in contrast to APOBEC3G(49-51). In any event, we also found that MORC2 was dispensable for Vpx-mediated HUSH or Vpr-mediated HLTF degradation. Altogether, we could not find any evidence that MORC2 is targeted by Vpr or Vpx and the question of whether MORC2 evolution has been driven by lentiviruses remains open.

Because MORC2 can operate with HUSH, studying Vpr/Vpx impact on MORC2 seemed logical to us. Nonetheless, we also provide several lines of evidence suggesting that MORC2 could act independently from HUSH: (i) as already stated, MORC2 presents sites of positive selection, not the HUSH components, (ii) MORC2, in contrast to HUSH, is not targeted by Vpx to the degradation pathway, (iii) MORC2 still maintains a repressive effect following TASOR depletion post-infection, (iv) MORC2 is detected in quiescent CD4+ T cells, not the HUSH subunits, (v) in addition, MORC2 was found at

Transcription Start Sites (TSS) in the absence of HUSH(11), in line with our finding of MORC2 being on the HIV-1 promoter and not on the coding sequence. Regardless of whether MORC2 works with HUSH, it may be that MORC2's sites of positive selection result from the MORC2's engagement in an evolutionary arms race with a wide variety of entities other than lentiviruses. The viruses of interest are those replicating *via* a DNA intermediate, present in the nucleus and silenced by repressive epigenetic marks, such as from the *Herpesviridae* family, like Herpes simplex virus-1 (HSV-1)(52) or Cytomegalovirus (CMV)(53), or from the *Hepadnaviridae* family, like Hepatitis B Virus (HBV)(54). Recently, the ICP0 protein encoded by HSV-1 has been identified as a viral antagonist of MORC3, another member of the MORC family also involved in gene silencing and regulation of chromatin structure(55-58), highlighting *Herpesviridae* antagonists as potential drivers of the evolution of MORCs. The molecular conflict might also involve young and potentially adapting retroelements that are under the control of HUSH(31, 59-62). Finally, MORC2 may also have evolved under the selection process underlying speciation and adaptation as is the case for several other transcription factors or chromatin-associated proteins(63). It is today impossible to predict which field will lead to the discovery of the drivers of the herein-identified MORC2 adaptive evolution, i.e. which are the proteins undergoing coevolution with MORC2.

Ironically, while Vpx induces HUSH degradation, MORC2 is stabilized in the presence of Vpx, due to a transcriptional effect: MORC2 gene expression being repressed by HUSH, the degradation of HUSH by Vpx induces an increase of MORC2 mRNA levels and subsequently of MORC2 protein levels(23). This stabilization effect at the protein level, previously reported in(4), is also seen when cells are infected with a complete wt HIV-2 virus compared to the ΔVpx virus. This result led us to wonder whether MORC2 could be mobilized to repress the provirus once HUSH is degraded. This hypothesis is supported by the finding that MORC2 seems able to maintain the repression of an integrated provirus following TASOR depletion, although we cannot rule out the possibility that a small amount of remaining TASOR is sufficient to repress the provirus in association with MORC2. MORC2 might provide a feedback control mechanism by limiting access of the HIV-1 LTR to transcription factors once TASOR is depleted. Indeed, MORC2 recruitment to gene promoters and to TSS was described to be HUSH-independent(11). It would be further interesting to quantify the HIV-1 LTR methylation modification upon HUSH depletion, as MORC2 is involved in the repression of endogenous genes by inducing methylation of promoters through the recruitment of DNMT3A(64). In line with this idea, gene silencing by RNA-directed DNA methylation in *Arabidopsis thaliana* depends on MORC proteins(65). Finally, we found that only MORC2 is expressed in quiescent CD4+ T cells, suggesting that while HUSH and MORC2 would together be involved in establishing HIV-1 latency, MORC2 alone might later also be involved in maintaining this provirus repression once activated CD4+ T cells return to a quiescent state. Our results in two HIV-1 models of latency further suggest that MORC2 could be involved in this process. Altogether, these observations suggest that MORC2 could act as an immune gatekeeper following the degradation of HUSH, in particular during HIV-2 infection. Strikingly, with a different mechanism, MORC3 was proposed as a gatekeeper of its own anti-viral function: by degrading MORC3, HSV-1 unleashes the second antiviral activity of MORC3, which is the repression of the *IFNB1* gene expression and, subsequently, induces interferon production(57).

How MORC2 operates mechanistically is still poorly understood. MORC2 possesses a chromatin remodelling activity associated to its ATPase domain. Here, we also show that MORC2, like TASOR, acts directly or indirectly at the post-transcriptional level, that it is found in complex with CNOT1 in an RNA-dependent manner and synergistically cooperates with the latter to repress LTR-driven transcription. MORC2 also interacts with proteins from the TRAMP-like PAXT complex, ZFC3H1 and MTR4, further supporting the hypothesis of a role of MORC2 in RNA destabilization. This is consistent with MORC2 working with TASOR and reinforces the idea of an integrated process linking epigenetic regulation and RNA metabolism to control gene expression. A specific chromatin environment or intrinsic properties of HUSH target genes, might explain the need for HUSH to recruit MORC2. Namely, HUSH was reported to specifically target intronless genes(66). Other ATPases play a key role in chromatin organization and dynamic, like SMC (Structural Maintenance of Chromosomes) proteins(67, 68). Though the ATPase domain differs between SMC and MORC proteins, both dimerize and mediate DNA binding, and it could be that MORC2 functions similarly to SMC proteins. Strikingly, the SMC5/6 complex silences unintegrated HIV-1 DNA and is antagonized by HIV-1 Vpr(69, 70), as well as by HBV and hepadnaviral X proteins (71-73), highlighting how silencing by chromatin remodelling proteins may represent an important barrier against the propagation of viruses. Whether MORC2 is required for the recruitment of the PAXT complex and the exosome by HUSH, and vice-versa, remains also to be investigated. The mechanism of MORC2-mediated silencing in the absence of HUSH is also unknown: MORC2 might act at the post-transcriptional level independently of HUSH, as suggested for the close related MORC3 protein(56). Whether MORC2 cooperates with CNOT1 once HUSH is depleted remains a possibility since MORC2 and CNOT1 still interact in the absence of TASOR. These questions are of paramount importance since MORC2 only, and not HUSH components, are detected in quiescent CD4+ T cells, highlighting MORC2 as a potential key player in the persistence of the virus in HIV-infected individuals.

Materials and Methods

Sequence and evolutionary analyses

The sequences of primate orthologous genes of MORC2 were retrieved from publicly available databases using NCBI Blastn, UCSC Blat or Ensembl, with the human sequence as the query. For phylogenetic and positive selection analyses, we retrieved one coding sequence per primate species for a total of 25 species. For each gene, two datasets were independently analyzed: one included the entire primate evolutionary history (spanning approximately 87 million years of primate evolution) and one was restricted to the simian primate species (spanning approximately 40 million years; with 21 simian primate species included). Orthologous sequences were codon-aligned using Muscle v3.8(74) and the phylogenetic tree was built using PhyML v3(75) with a HKY+I+G model with 1,000-bootstrap replicates for statistical support.

To comprehensively determine the evolution of MORC2 in primates, we performed positive selection analyses. Maximum-likelihood tests to assay for positive selection were performed using three packages: HYPHY v2.3(76), PAML v4(77) and Bio++ v2.2.0 , all available within the DGINN pipeline(23,

78). In HYPHY, we used the branch-site unrestricted statistical test for episodic diversification (BUSTED) method, which detects gene-wide evidence of episodic positive selection within a codon alignment. In PAML, we used the Codeml program with the corresponding gene tree inferred from PhyML as input. Parameters were checked using the M0 one ratio model and the sequence alignments were then fit to models that disallow (M1 and M7) or allow (M2 and M8) positive selection. Likelihood ratio tests (LRTs) were performed to compare model M1 versus M2 and M7 versus M8, using a $\chi 2$ test to derive P values. We finally used the Bio++ package to similarly test for evidence of positive selection ($M1^{NS}$ versus $M2^{NS}$ and $M7^{NS}$ versus $M8^{NS}$, as implemented in Bio++; NS for non-stationary models). To look more specifically for site-specific positive selection, we used the fast, unconstrained Bayesian approximation for inferring selection (FUBAR) method from HYPHY/Datamonkey. In Codeml and Bio++, we used Bayesian empirical Bayes (BEB) analyses and Bayesian posterior probabilities, respectively, from the M2 and M8 models to determine if any codon was under significant positive selection.
Protein structure representations were conducted using UCSF Chimera (The Regents) software. Protein structure predictions are from AlphaFold Protein Structure Database(79).

Plasmids and transfection

MORC2 expression vectors pCMV6-myc-DDK, pCMV6-MORC2-myc-DDK have been purchased from Origene. pCMV6-MORC2-myc-DDK vector expresses MORC2 isoform 1 of 1032 amino acids (NCBI Reference Sequence: NP_001290185.1). MORC2-R252W and MORC2-D68A constructs were obtained by directed mutagenesis using Phusion High Fidelity DNA polymerase (Thermo-Fisher) and following 5′-3′-oriented primers F-CTCTATATTGATCCCTGGATGAGGATCTTC/ R-AAGATCCTCATCCAGGGATCAATATAGAG to raise the R25W mutant and F-GTTATGTTTTTTGGCTGATGGAGCAGG / R-CCTGCTCCATCAGCCAAAAAACATAAC to raise the D68A mutant. The pCMV6-MORC2-myc-DDK plasmid encoding the MORC2 cDNA from *Macaca mulatta* (rhesus macaque, NCBI Reference Sequence: NP_001248528.1), *Otolemur garnettii* (Northern greater galago, NCBI Reference Sequence: XP_003803380.2) and *Cebus capucinus imitator* (white-faced capuchin, NCBI Reference Sequence: XP_017355058.1) have been synthesized by Genecust through gene editing strategy.
The pLentiCRISPRv2-sgMORC2-Cas9 was obtained by subcloning the following 5′-3′-oriented annealed primers: F-CACCGAGTAGACTCAGGTGTTCGCT / R-AAACAGCGAACACCTGAGTCTACTC, containing the sgRNAs targeting the 5^{th} exon of MORC2, with the enzyme BsmBI. For complementation assays, pCMV6-MORC2-myc-DDK was made resistant to the guide by mutating the sgRNA-targeted sequence with 5′-AAGCGAACACCTGAGTCTACT-3′. pLentiCRISPRv2-sgTASOR-Cas9 was obtained by subcloning the following 5′-3′-oriented annealed primers: F-CACCGCTTTCCCAACTCGCATC CGT / R-AAACACGGATGCGAGTTGGGAAAGC, containing the sgRNAs targeting the first exon of TASOR, with the enzyme BsmBI.
All plasmids are transfected in cells by the calcium-phosphate co-precipitation method.

Virus and VLP production

All Virus Like Particles (VLP) and most of the viruses were pseudo-typed with VSV-G protein and produced in the 293 FT cell line (Gift from Nicolas Manel) through the calcium-phosphate co-precipitation method. Cell culture medium was collected 48h after transfection and filtered through 0.45 µm pore filters. Viral particles or VLPs were concentrated by sucrose gradient followed by ultra-centrifugation.

Regarding VLP production with viral proteins expressed in trans, SIV3+ ΔVprΔVpx packaging vector (a gift from N. Landau(80)) and a VSV-G vector were co-transfected with pAS1B-HA-Vpx HIV-2 Ghana or pAS1B-HA (empty) in order to produced VLP containing HA-tagged Vpx protein. In the same manner pPAX2 packaging HIV-1 were co-transfected with a VSV-G vector and pAS1B-HA-Vpr HIV-1 or pAS1B-HA (empty) in order to produce VLP containing HIV-1 Vpr protein. With respect to VLP with viral proteins expressed in cis, we transfected with the VSV-G vector, the SIV3+ ΔVprΔVpx packaging vector (as the empty condition) or SIV3+ WT (R+X+ condition)(81) in order to produce VLP containing all accessories proteins encoded by the SIV3+ vector.

To deliver the sgRNAs and Cas9 into the target cell to knock out MORC2, TASOR or Mock (control): pPAX2 packaging vector was co-transfected along with pLentiCRISPRv2-sgTASOR-Cas9, or with pLentiCRISPRV2-sgMORC2-Cas9 or with pLentiCRISPRV2-Cas9 (control) for VLP production (with VSV-G).

To produce HIV-1 viral particles: pPAX2 packaging was co-transfected with the HIV-1 LTR-eGFP transfer vector, described in(4) and obtained from Addgene (plasmid # 115809) to produce the HIV-1 LTR-eGFP virus, or with the pCTS.Luc transfer vector (a gift from Stéphane Emiliani) to produce HIV-1 LTR-CMV-Luc-LTR virus (with VSV-G).

HIV-1 (Sup. Fig. 1) and HIV-2 (Fig. 2A) replicative viruses pseudo-typed VSV-G were produced by transfection of pNL4.3 WT or pGLAN WT (gift from Akio Adachi(82)) and VSV-G vectors and titered on the HeLa TZMbl reporter cell line. HIV-2 ΔEnv-luciferase viruses, deleted of the Env gene and with luciferase in place of Nef, were obtained following transfection of pGLANΔEnv luciferase (also a gift from Akio Adachi(83)) and VSV-G vectors.

Cell lines

HeLa (CCL-2) and HEK293T (CRL-3216) cells were cultured in media from ThermoFisher DMEM and Jurkat (TIB-152) and J-Lat A1 cells were cultured in media from ThermoFisher RPMI containing 10% heat-inactivated fetal bovine serum (FBS, Dominique Dutscher), 1000 units/mL penicillin, and 1000 µg/mL streptomycin.

HeLa KO CTRL, KO TASOR and KO MORC2 cells were generated by the transduction of HeLa cells by VLP containing CRISPR-sgRNA-Cas9 construct targeting respectively TASOR and MORC2 genes. Three days after transduction, these cells were treated by puromycin (1mg/mL) during 5 days. After selection, these cells were diluted and plated in 96-well plates in order to obtain a single cell per well and thus to make a clonal selection. After clonal amplification, MORC2 and TASOR protein levels in each different clone were checked by western blot.

The HIV-1 latency model J-Lat A1 was generated and described by Jordan et al.(37). J-Lat A1 KO Control (CTRL) and MORC2 KD cells were generated by transfection of pLentiCRISPRv2-sgCtrl-Cas9

and pLentiCRISPRv2-sgMORC2-Cas9 respectively, with DMRIEC reagent. Transfected cells were cultured for 3 days prior to puromycin selection (1µg/mL during 3 days). The J-Lat A1 MORC2 KD cells were sorted by flow cytometry with the BD FACS ARIA3 cytometer of CYBIO platform (Institut Cochin) to separate three populations of cells: GFP-negative cells, GFP-positive-cells with low GFP expression (Dim) and GFP-positive cells exhibiting high GFP expression (Bright). Cells were then amplified for two weeks in culture before subsequent experiments.

The Jurkat cell line was infected with HIV-1-LTR-eGFP(4) and then the eGFP positive cells were sorted by flow cytometry with the BD FACS ARIA3 cytometer of the CYBIO platform (Institut Cochin). After 2 weeks of culture, a second sorting was performed to recover the cells that had become eGFP negative. Jurkat latently infected HIV-1-eGFP were transfected by pLentiCRISPRv2-sgCtrl-Cas9 and pLentiCRISPRv2-sgMORC2-Cas9 with DMRIEC reagent in order to generate HIV-1-LTR-eGFP KD Ctrl or KD MORC2 Jurkat cells respectively.

HeLa LTR-ΔTAR-Luc cells were generated in the laboratory of Stéphane Emiliani from the HeLa LTR-Luc cells described in(84).

PBMCs from the blood of anonymous donors (obtained in accordance with the ethical guidelines of the Institut Cochin, Paris and Etablissement Français du Sang) were isolated by Ficoll (GE Healthcare) density-gradient separation. CD4+ T cells were isolated by positive selection (using magnetic CD4 human MicroBeads from Miltenyi Biotec). Cells were activated with CD3/CD28 agonists (T Cell transact) and stimulated with human IL-2 (50u/mL) for 3 days. Cells were then washed twice with Dulbecco's PBS 1x and lysed with RIPA buffer to assess TASOR and MORC2 protein levels by Western-Blot.

siRNA treatment

HeLa cells were transfected by siRNA with DharmaFECT1 (Dharmacon, GE Lifesciences). The final concentration for all siRNA was 100 nM. The following siRNAs were purchased from Sigma Aldrich: siMORC2: SASI_Hs01_0097055; siTASOR: SASI_Hs02_00325516; siCNOT1: SASI_Hs02_00349201. And siDCAF1: GGAGGGAAUUGUCGAGAAU from Dharmacon. The non-targeting control siRNAs (MISSION siRNA Universal Negative Control #1, SIC001) were purchased from Sigma Aldrich.

Luciferase activity assays

Cells were washed twice with Dulbecco's PBS 1x then lysed with the lysis buffer cell culture Lysis Reagent 1X from Promega and centrifugated 10 min at 15000g. Luciferase activity was measured using a luciferase assay system from Promega and a TECAN multimode reader Infinite F200 Pro. Luciferase activity data was normalized on protein concentration with the use of Pierce BCA Protein Assay Kit (232255, Thermo-Fisher).

Flow cytometric analysis

J-Lat A1 and Jurkat cells were collected and washed with PBS and resuspended in PBS-EDTA 0,5 mM. Data was collected and analyzed with a BD Accuri C6 cytometer and software CFlow Plus. At least 10,000 events in P1 were collected, the GFP-positive population was determined using a GFP-negative

population when possible (for Jurkat cells) or arbitrary (as for J-Lat cells) and the same gate was maintained for all conditions. Analysis was performed on the whole GFP-positive population.
Regarding reactivation assay, Jurkat cells are reactivated with 1 ng/mL of TNF-α.

Chromatin immunoprecipitation

HeLa LTR-ΔTAR-Luc cells were grown in 10 cm dishes and transfected with Flag-Empty or MORC2-Flag plasmids and a GFP plasmid with CaCl2. 48h after transfection, $10x10^6$ cells of each condition were collected, fixed in 1% paraformaldehyde (043368.9M, ThermoFisher) at room temperature (RT) for 30min and then quenched with glycine 0.125M (C01010062, Diagenode) at RT for 10min. Cells were then washed twice in PBS and pellets were lysed by freezing in -80°C. Meanwhile, 52µL of Protein G beads (10004D, Invitrogen) were washed once with 300µL of ChIP buffer (SDS 0.1%, Triton 1.1%, 1.2mM EDTA, 16.7mM Tris HCl pH 8, 200mM NaCl) on magnetic rack and then resuspended in 300µL of ChIP buffer and 3µg of anti-Flag antibody (F1804-200UG, Merck) before being placed on wheel for 1h at RT. Lysed cells were resuspended in 500µL of Sonication buffer (SDS 1%, 10mM EDTA, 50mM Tris HCl pH 8) with an anti-protease cocktail (A32965, ThermoFisher) and sonicated for 15" at 4°C (30s ON, 30s OFF) with a Diagenode BIORUPTOR Pico. After clarification of the sonicate by centrifugation, 100µL were collected for inputs and diluted with 100µL of ChIP buffer. The remaining 400µL were transferred to a new tube and 150µL of bound antibody was then added to each condition before being wheeled overnight at 4°C. The next day, beads were washed once with a Low Salt buffer (SDS 0.1%, Triton 1%, 2mM EDTA, 20mM Tris HCl pH 8, 150mM NaCl), once with a High Salt buffer (SDS 0.1%, Triton 1%, 2mM EDTA, 20mM Tris HCl pH 8, 500mM NaCl), once with a LiCl buffer (0.25M LiCl, NP-40 1%, 1mM EDTA, 10mM Tris HCl, 1% Deoxycholate) and twice with PBS. Beads were then eluted twice with 100µL of Elution buffer (SDS 1%, 0.1M NaHCO3) for 30min at RT; the eluate was transferred to a new tube. Then, 1µL of Proteinase K (EO0491, ThermoFisher) was added for each condition and inputs as well and incubated for 30min at 55°C. DNA was then purified by adding 200µL of Phenol/Chloroform/Isoamyl alcohol (25:24:1) (327115000, ThermoFisher), vortexing and centrifuging at maximum speed for 15min at RT. The upper phase was then transferred into a new tube and 0.5 volume of NH4OAc, 1µL of glycogen and 2.5 volume of 100% ethanol were added to precipitate DNA; then, after vortexing, tubes were incubated at -80°C for 1h. Then, after 30min of centrifugation at maximum speed, 4°C and two washes with 70% ethanol, pellets were air-dried for 5min before resuspension in 80µL of DNAse free water. qPCR was finally performed as described in the RT-qPCR section.

Nuclear Run On (NRO)

HeLa LTR-ΔTAR-Luc cells were plated in 10 cm dishes at 2,5 billion cells and the following day transfected with siRNA CTRL, TASOR + CTRL and MORC2 + CTRL at a final concentration of 100 nM each. NRO was performed as precisely described by Roberts and colleagues(85), except for these specific points: At step 14, RNA extractions with rDNase treatment were performed with NucleoSpin RNA, Mini kit (740955.250, Macherey-Nagel). At Step 44, Reverse transcription was performed with Maxima First Strand cDNA Synthesis Kit with dsDNase (K1672, ThermoFisher). qPCR was finally performed as described in the RT-qPCR section.

RT-qPCR

RNA extractions were performed through NucleoSpin RNA, Mini kit (740955.250, Macherey-Nagel). Reverse transcription steps were performed with Maxima First Strand cDNA Synthesis Kit with dsDNase with 1µg of total RNA. qPCRs were performed thanks to a LightCycler480 (Roche) using a mix of 1x LightCycler 480 SYBR Green I Master (Roche) and 0.5 µM primers. The sequences of 5'-3' oriented primers are as follows: Nuc0: F-ATC TAC CAC ACA CAA GGC TAC / R-GTA CTA ACT TGA AGC ACC ATC C; Enh: F-TGA GCC TGC ATG GAA TGG AT / R-CCA GCG GAA AGT CCC TTG TA; Enh w/o AP1: F-CCT TTG GAT GGT GCT ACA AGC / R-AAT GCT AGG CGG CTG TCA AA; Nuc1: F-AGT AGT GTG TGC CCG TCT GT / R-TTG GCG TAC TCA CCA GTC GC; Luc 5': F-AAG AGA TAC GCC CTG GTT CCT / R-CGG TAG GCT GCG AAA TGT TCA; Luc 3': F-CTC ACT GAG ACT ACA TCA GC/ R-TCC AGA TCC ACA ACC TTC G; Tug1: F-GAC TCC CTT AAG CAA CAC CAG A / R-GAG CCC CTT TAG GAA ATG TTG C; ZNF224: F-TGG GAA GAG TTT TGG CTG GG / R-TGG GTC AGA CGA GTT GAG GA; GFP: F-GGT GTT CTG CTG GTA GTG GT / R-TCG AGG GCG ACA CCC TG; ; MORC2: F-ACT GGA CAG CCT CCA AGA GA / R-TCC TGG CAG ATT GCT CAC AT; GAPDH: F-ATG GGG AAG GTG AAG GTC G / R-AGT TAA AAG CAG CCC TGG TG; 18S: F-GTA ACC CGT TGA ACC CCA TT / R-CCA TCC AAT CGG TAG TAG CG.

Cell fractionation and Immunoprecipitation

All immunoprecipitation experiments are performed in the nuclear fraction of HeLa cells (WT, KO CTRL, KO MORC2 and KO TASOR). HeLa cells grown in 10 cm dishes were washed with cold Dulbecco's PBS 1x (ThermoFisher). After trypsinization (25200056, Thermo- Fisher), cells were recovered in 1.5 mL tubes and washed once with ice-cold PBS. After 4 min of centrifugation at 400xg, 1 mL of Cytoplasmic Lysis Buffer
(10 mM TRIS-HCl pH7.5, 10 mM NaCl, 3 mM MgCl2, and 0.5% IGEPAL® CA-630 (I8896-100ML-Merck)) was added on the cell pellet and resuspended pellet was incubated on ice for 5 min. Cells were then centrifuged at 300 × g for 4 min at 4 °C. The supernatant was saved for cytoplasmic fraction. The pellet was resuspended with 1 mL of Cytoplasmic Lysis Buffer and re-centrifuged at 300 × g for 4 min at 4 °C twice. Finally, the nuclear pellet was lysed with 300 µL of RIPA Buffer. 250 µg of nuclear proteins was incubated with 3µg of anti-IgG antibody or 3µg of anti-CNOT1 antibody or 3µg of anti-MORC2 or 3µg of anti-DDK at 4°C under overnight rotation. The following day, with pre-washed PierceTM Protein A/G Magnetic Beads (88802, ThermoFisher) were added to the samples for 1h at room temperature. The captured beads were washed 3 times with the wash buffer (150mM NaCl, 50mM Tris pH7,5). Finally, elution was performed by adding 1x Laemmli solution containing DTT 0,1M and heated for 10 min at 95°C.

Western-Blot and antibodies

For all lysates, the proteins were separated through precast 4-12 % Bis-Tris gradient gels from ThermoFisher. Then proteins were transferred onto PVDF membrane (ThermoFisher: 88520). Finally, proteins were revealed by immunoblot. The following antibodies, with their respective dilutions in 5%

skimmed milk in PBS-Tween 0.1%, were used: anti-TASOR (HPA017142 Merck) 1/1000, anti-MORC2 (PA5-51172, TermoFisher) 1/1000, anti-CNOT1 (For WB: 66507- 1-Ig Proteintech, 1/1000; For IP: 14276-1-AP, Proteintech), β-actin (AC40, A3853, Merck) 1/1000, anti-GFP (11814460001, Roche), anti-Flag-M2 (F1804-200UG Merck) 1/1000, anti-MPP8 (HPA040035 Merck) 1/1000, GAPDH (6C5, SC-32233, Santa Cruz) 1/1000, anti-DCAF1 (11612-1AP, Proteintech), anti-HLTF (ab17984, Abcam) 1/1000, anti-α-tubulin (T9026-.2mL Merck) 1/1000, anti-SUPT6H (23073-1-AP, Proteintech), anti-MTR4 (12719-2-AP, Proteintech), anti-YTHDF2 (24744-1-AP, Proteintech), anti-NONO (11058-1-AP, Proteintech), anti-ZFC3H1 (HPA007151-100UL, Merck). Anti-p27/p55 and anti-P24 were provided by the NIH AIDS research and reference reagent program (ref ARP392/393) 1/1000. All secondary antibodies anti-mouse (31430, lot VF297958, ThermoFisher) and anti-rabbit (31460, lots VC297287, UK293475 ThermoFisher) were used at a 1/10000 dilution before reaction with Immobilon Forte Western HRP substrate (WBLUF0100, Merck Millipore). Signals were acquired with Fusion FX (Vilber).

Data and Reagent availability.

Data for sequence analyses (codon alignments, and phylogenetic tree) are available at https://doi.org/10.6084/m9.figshare.22337539 , https://doi.org/10.6084/m9.figshare.22337542 , and https://doi.org/10.6084/m9.figshare.22337545. All other data and reagents are available from the corresponding authors.

Acknowledgements and funding sources

We thank all the members of the Retrovirus, Infection and Latency group, Stéphane Emiliani and Sarah Gallois-Montbrun at Institut Cochin for fruitful discussions. We also thank the members of the LP2L team at CIRI, Lyon, for support. We acknowledge the CYBIO and GENOM'IC platforms of the Institut Cochin.

This work was supported by grants from SIDACTION, the "Agence Nationale de la Recherche sur le SIDA et les hépatites virales" (ANRS) and Fondation pour la Recherche Médicale (FRM, PROJECT EQU202203014684 atttibuted to F.MG.). R.M. was supported by SIDACTION and FRM ; M.M.M. by SIDACTION ; A.L., S.M. and P.L. by Université de Paris Cité ; V.V. by ANRS. This work in the laboratory of L.E. is supported by grants from the French Research Agency on HIV and Emerging Infectious Diseases ANRS/MIE (#ECTZ118944 to LE) and the Sidaction (n°21-1-AEQ-12972-2 to LE and FMG). AL is supported by a PhD fellowship from Sidaction (2020 - n°12673). LE and AC are supported by the CNRS.

Figure legends

Figure 1: MORC2 presents signatures of positive selection during primate evolution and anti-lentiviral/HIV activity

A. Phylogenetic analysis of primate MORC2. The tree was built with PhyML and statistical support is from 1,000 bootstrap replicates (asterisks correspond to bootstrap values >0.75). The scale bar indicates the number of substitutions per site. Four black arrows correspond to the orthologous MORC2s

that were subsequently tested in functional assays. **B. Evidence of positive selection during primate MORC2 evolution.** Analyses were performed with the DGINN pipeline, using the primate and the simian codon alignments at the gene-wide level (from 25 and 21 species, respectively). We used five methods to assess for positive selection: BUSTED from HYPHY, as well as two analyses from PAML CodeML and from Bio++ (see methods). P values that support a model allowing for positive selection are shown in parentheses. **C. Sites under positive selection in primate MORC2**. Site-specific positive selection analyses were performed using the DGINN pipeline and the Datamonkey server: MEME and FUBAR, BEB from PAML Codeml M2 and M8, and PP from Bio++ M8. Only the sites above the indicated "statistically significant cut-off" are shown. In bold are the sites identified by several methods. **D. Amino acid alignment of the sites under positive selection.** The species correspond to the panel A. Coloring is according to RasMol (Geneious, Biomatters). **E. Schematic of MORC2 with its functional domains and the herein identified sites under positive selection**. The ATPase module contains the ATPase domain, the coiled-coil domain 1 and the S5 domain. CC: Coiled-coil domain, CW: CW domain with zinc finger, CD: Chromodomain. Sites under positive selection from primate and simian analyses are indicated by red crosses. **F. Predictive 3D structure representation of MORC2 domains and sites under positive selections.** AlphaFold structure prediction of human MORC2. Functional domains are coloured following the panel E colour code. Atoms of the residues under positive selection are coloured in red and represented with sticks. Corresponding coordinates are labelled in red. **G. Depletion of MORC2 favors HIV-1- and SIVmac-derived virus expression**. HeLa cells were infected by HIV-1- or SIVmac-derived viruses expressing luciferase (luc) (LTR-CMV-Luc viruses), then the following day, treated during 72h by siRNA CTRL or three (or two) different siRNA MORC2. Luc gene expression was measured by Luc activity assay ($n = 3$; each replicate is presented along with the mean values and the SEM. A two-sided unpaired *t* test was used. *$p = 0.05$ **$p = 0.01$ ***$p < 0.001$) **H. Overexpression of human and orthologous primate MORC2 proteins induces a decrease of HIV-1-derived virus expression.** HeLa KO MORC2 cells were infected by HIV-1 LTR-CMV-Luc viruses, then the following day, transfected by vectors expressing different MORC2 proteins (four orthologous proteins from divergent primate species: human (Hu), rhesus macaque (Mac), Northern greater galago (Lem), white-faced capuchin (Cap)); MORC2 D68A, an ATPase defective protein, used as a control; and MORC2 R252W, which is the protein produced by a mutated *MORC2* gene in the Charcot Marie-Tooth disease and which is supposed to hyperactivate HUSH. Luc gene expression is measured by Luc activity assay (Minimum $n = 4$; each replicate is presented along with the mean values and the SEM. A two-sided unpaired *t* test was used. **$p = 0.0023$ ***$p = 0.0002$ ****$p < 0.0001$).

<u>Figure 2:</u> MORC2, in contrast to HUSH, is not degraded, but is stabilized by full length HIV-2, thanks to Vpx

A. HUSH degradation upon HIV-2 infection is accompanied by a slight increase in MORC2 levels. Jurkat T cells were non-infected (NI) or infected with complete HIV-2 viruses (WT), or HIV-2 viruses deleted of either Vpr (ΔR), Vpx (ΔX) or both (ΔRΔX). Levels of the indicated proteins were analyzed by western blot. **B. MORC2 levels are upregulated in the presence of Vpx from HIV-2 or from SIVsmm.** HeLa cells were treated by HIV-2 or SIVsmm Vpx-containing VLPs. Cells were lysed 24h post-

transduction and Western-Blot was performed. **C. MORC2 is not required for Vpx-mediated HUSH degradation.** HeLa cells were treated by siRNA against MORC2, then transduced by VLP containing Vpx. **D. MORC2 can maintain HIV-1 repression after TASOR degradation by Vpx.** HeLa cells were infected by the HIV-1 LTR-CMV-Luc virus, 2 days later, TASOR was depleted by Vpx, then the following day, MORC2 was depleted by siRNA. Luciferase gene expression is measured by Luciferase activity assay ($n = 3$ each replicate is presented along with the mean values and the SEM. A two-sided unpaired *t* test was used. $^{**}p = 0.0036$ $^{***}p < 0.0001$). **E. The silencing of an incoming virus by MORC2 needs TASOR and *vice versa*.** *Left*. TASOR-depleted cells (or Control cells) were infected with the HIV-1-derived virus (LTR-CMV-luc), then 2 days later, MORC2 was silenced by siRNA. Luciferase gene expression was measured by Luciferase activity assay ($n = 3$; each replicate is presented along with the mean values and the SEM. A two-sided unpaired *t* test was used. $^{**}p = 0.009$). *Right.* MORC2-depleted cells (or Control cells) were infected with the HIV-1-derived virus (LTR-CMV-luc), then 2 days later, TASOR was depleted by Vpx. Luciferase gene expression was measured by Luciferase activity assay ($n = 3$; each replicate is presented along with the mean values and the SEM. A two-sided unpaired *t* test was used. $^{***}p = 0.0004$).

Figure 3: MORC2 destabilizes HIV-1 LTR-driven transcripts and cooperates with CNOT1.
A. MORC2 binds the HIV-1 LTR promoter. MORC2 occupancy was measured by ChIP-qPCR in cells transfected for 72h with Flag-Empty or MORC2-Flag plasmids together with a GFP-encoding vector. Immunoprecipitations were performed with an anti-Flag antibody and sonicated DNA was amplified with specific primers: either mapping to the HIV provirus as depicted at the top (left), or mapping to host genes; Tug1 and ZNF224 are HUSH target genes. Data are mean of n=5 biological replicates + SEM. **B. MORC2 negatively impacts LTR-driven transcripts at both transcriptional and post-transcriptional levels**. HeLa HIV-1 LTR ΔTAR-Luc cells were transfected for 72 h with Ctrl or MORC2 siRNA. Nuclear Run On experiments were performed to analyze the effect of MORC2 depletion on the level of nascent and total RNAs from the LTR *(Bottom).* Western Blot was performed to check the depletion of MORC2 and TASOR *(Top)*. **C. MORC2, CNOT1 and TASOR cooperate to repress expression from the HIV-1 LTR.** HeLa HIV-1 LTR ΔTAR-Luc cells were transfected for 72 h with one or two or three siRNAs as indicated. Luc activity *(Left)* was measured ($n = 3$; each replicate is presented along with the mean values and the SEM. A two-sided unpaired *t* test was used. $^{**}p < 0.01$ $^{***}p < 0.001$ $^{****}p < 0.0001$) and protein depletion was checked by Wester-Blot *(Right).* **D. MORC2 interacts with CNOT1 in a RNA-dependent manner.** Nuclear fraction of HeLa cells was isolated and incubated with RNAse or not for 30 minutes at room temperature. Then, endogenous CNOT1 or MORC2 were immunoprecipitated with specific antibodies as indicated and Western-Blot performed. The cytoplasmic GAPDH protein is a control of the nucleus-cytoplasm fractionation. **E. MORC2 WT and MORC2 ΔCD interact similarly with CNOT1 and the PAXT complex.** MORC2-DDK WT and MORC2-DDK ΔCD encoding vectors and the corresponding empty vector were transfected in HeLa cells. After 48h, cells were lysed and the nuclear fraction was isolated. Anti-DDK immunoprecipitation on this nuclear fraction and Western Blot were performed.

Figure 4: MORC2 presents a repressive effect in two models of HIV-1 latency

A. MORC2, but not TASOR, is expressed in non-activated CD4+ T cells. Human naïve T cells were isolated from four blood donors. These cells were activated by anti-CD3 and anti-CD28 antibodies. Three days after this co-stimulation, cells were harvested. Lysates of non-activated and activated cells were probed for the presence of MORC2 and TASOR by western-blot. **B. MORC2 represses HIV-1 expression in the J-Lat A1 model of latency.** *Left*. J-Lat A1 cells, harboring one copy of integrated latent LTR-tat-*IRES*-GFP-LTR construct, were depleted of MORC2 by Crispr/Cas9, which leads to an increase of the percentage of GFP-positive cells (reactivation of the virus analyzed by cytometry). *Right.* MORC2 depletion accompanies viral reactivation gradually. J-Lat A1 Cells were FACS-sorted according to GFP expression. More LTR-driven GFP expression was high, less MORC2 was expressed. **C. MORC2 represses HIV-1 LTR-driven EGFP expression in latently infected Jurkat T cells.** Jurkat T cells latently infected by HIV-1-eGFP (the viral genome is schematically shown above) were depleted of MORC2 by Crispr/cas9, which leads to enhanced HIV-1 expression without and with TNFα.

Supplementary Figure 1: MORC2 does not appear counteracted by HIV-1 Vpr

A. TASOR depletion induces an increase of MORC2 mRNA level. HeLa HIV-1 LTR ΔTAR-Luc cells were transfected by Ctrl or TASOR siRNA and, 72h post-transfection, cells were lysed and RT-qPCR was performed to analyze mRNA MORC2 levels ($n = 3$; each replicate is presented along with the mean values and the SEM. A two-sided unpaired *t* test was used). **B. HIV-1 does not induce MORC2 protein depletion.** Jurkat T cells were non-infected (NI) or infected with complete HIV-1 viruses (WT) or HIV-1 viruses deleted of Vpr (ΔR), at two different MOI (0.1 and 0.5). Indicated proteins are revealed by western blot. HLTF protein is a positive control of depletion by Vpr-containing HIV-1. **C. Vpr and Vpx proteins from divergent primate lentiviruses do not impact MORC2 expression**. Viral proteins from divergent origins were delivered by VLP: Vpr from SIVagm.Vervet (ver), Grivet (gri), Sabaeus (sab), Tantalus (tan), Vpx from SIVsmm (infecting sooty mangabey), SIVmnd-2 (mandrill), SIVrcm.gab1 and SIVrcm.ng411 (2 strains infecting red-capped mangabey). **D. MORC2 is not required for HIV-1 Vpr-mediated HLTF degradation.** HeLa cells were treated by MORC2 siRNA, then transduced by VLP containing HIV-1 Vpr. Cells were lysed the day after, and western-blot performed. **E. MORC2 remains active following HIV-1 Vpr treatment.** HeLa cells were infected by the HIV-1 LTR-CMV-Luc virus, 2 days later, HIV-1 Vpr was delivered thanks to VLP transduction, then the following, MORC2 was depleted by siRNA. Luciferase gene expression was measured by Luciferase activity assay ($n = 3$; each replicate is presented along with the mean values and the SEM. A two-sided unpaired *t* test was used. $^{**}p < 0.01$).

Supplementary Figure 2: MORC2 does not repress WT HIV-2 and Vpx-depleted HIV-2 viruses.

HeLa cells were infected by WT HIV-2 or Vpx-depleted HIV-2, both expressing luciferase in the Nef gene, at five different MOI (0.1, 0.25, 0.4, 0.6, 0.8). Two days post-infection, cells were transfected by MORC2 or Ctrl siRNA. Three days post-transfection, cells were lysed. Luciferase activity assay and a Western were performed.

Supplementary Figure 3: MORC2 interacts with proteins from the RNA degradation pathway

A. CNOT1 interacts with MORC2 in the absence of TASOR, and with TASOR in the absence of MORC2, in the nucleus of HeLa cells. Nuclear fraction of Hela KO CTRL, KO MORC2 and KO TASOR cells was isolated. Endogenous CNOT1 was immunoprecipitated with an antibody specific to CNOT1 and Western-Blot was performed. GAPDH is a negative control for nuclear fraction isolation. **B. Interaction of endogenous TASOR or MORC2 with RNA metabolism proteins**. Nuclear fractions of HeLa cells were isolated and TASOR or MORC2 were immunoprecipitated with specific antibodies, then western blot was performed. GAPDH is a negative control for nuclear fraction isolation and NONO a positive control.

Supplementary Figure 4: Model confidence of MORC2 AlphaFold predicted structure.

Left. Model confidence of MORC2 AlphaFold predicted structure. pLDDT (predicted local distance difference test): Per-residue confidence score. *Right*. Predicted aligned error plot of MORC2 AlphaFold predicted structure. Dark green represents low distance error in Ångströms, light green represents high distance error. Figures are from AlphaFold Protein Structure Database website.

References

1. K. B. Einkauf *et al.*, Parallel analysis of transcription, integration, and sequence of single HIV-1 proviruses. *Cell* **185**, 266-282 e215 (2022).
2. G. Chougui *et al.*, HIV-2/SIV viral protein X counteracts HUSH repressor complex. *Nat Microbiol* **3**, 891-897 (2018).
3. E. J. D. Greenwood *et al.*, Promiscuous Targeting of Cellular Proteins by Vpr Drives Systems-Level Proteomic Remodeling in HIV-1 Infection. *Cell Rep* **27**, 1579-1596 e1577 (2019).
4. L. Yurkovetskiy *et al.*, Primate immunodeficiency virus proteins Vpx and Vpr counteract transcriptional repression of proviruses by the HUSH complex. *Nat Microbiol* **3**, 1354-1361 (2018).
5. M. D. Daugherty, H. S. Malik, Rules of engagement: molecular insights from host-virus arms races. *Annu Rev Genet* **46**, 677-700 (2012).
6. N. K. Duggal, M. Emerman, Evolutionary conflicts between viruses and restriction factors shape immunity. *Nat Rev Immunol* **12**, 687-695 (2012).
7. D. Enard, L. Cai, C. Gwennap, D. A. Petrov, Viruses are a dominant driver of protein adaptation in mammals. *Elife* **5** (2016).
8. I. A. Tchasovnikarova *et al.*, GENE SILENCING. Epigenetic silencing by the HUSH complex mediates position-effect variegation in human cells. *Science* **348**, 1481-1485 (2015).
9. R. Matkovic *et al.*, TASOR epigenetic repressor cooperates with a CNOT1 RNA degradation pathway to repress HIV. *Nat Commun* **13**, 66 (2022).
10. W. Garland *et al.*, Chromatin modifier HUSH co-operates with RNA decay factor NEXT to restrict transposable element expression. *Mol Cell* 10.1016/j.molcel.2022.03.004 (2022).

11. I. A. Tchasovnikarova *et al.*, Hyperactivation of HUSH complex function by Charcot-Marie-Tooth disease mutation in MORC2. *Nat Genet* **49**, 1035-1044 (2017).
12. O. M. Albulym *et al.*, MORC2 mutations cause axonal Charcot-Marie-Tooth disease with pyramidal signs. *Ann Neurol* **79**, 419-427 (2016).
13. Y. S. Hyun, Y. B. Hong, B. O. Choi, K. W. Chung, Clinico-genetics in Korean Charcot-Marie-Tooth disease type 2Z with MORC2 mutations. *Brain* **139**, e40 (2016).
14. P. Lassuthova *et al.*, Severe axonal Charcot-Marie-Tooth disease with proximal weakness caused by de novo mutation in the MORC2 gene. *Brain* **139**, e26 (2016).
15. T. Sevilla *et al.*, Mutations in the MORC2 gene cause axonal Charcot-Marie-Tooth disease. *Brain* **139**, 62-72 (2016).
16. X. Zhao *et al.*, MORC2 mutations in a cohort of Chinese patients with Charcot-Marie-Tooth disease type 2. *Brain* **139**, e56 (2016).
17. D. Q. Li, S. S. Nair, R. Kumar, The MORC family: new epigenetic regulators of transcription and DNA damage response. *Epigenetics* **8**, 685-693 (2013).
18. G. Moissiard *et al.*, MORC family ATPases required for heterochromatin condensation and gene silencing. *Science* **336**, 1448-1451 (2012).
19. W. A. Pastor *et al.*, MORC1 represses transposable elements in the mouse male germline. *Nat Commun* **5**, 5795 (2014).
20. L. Zhang, D. Q. Li, MORC2 regulates DNA damage response through a PARP1-dependent pathway. *Nucleic Acids Res* **47**, 8502-8520 (2019).
21. H. Y. Liu *et al.*, Acetylation of MORC2 by NAT10 regulates cell-cycle checkpoint control and resistance to DNA-damaging chemotherapy and radiotherapy in breast cancer. *Nucleic Acids Res* **48**, 3638-3656 (2020).
22. D. Q. Li *et al.*, MORC2 signaling integrates phosphorylation-dependent, ATPase-coupled chromatin remodeling during the DNA damage response. *Cell Rep* **2**, 1657-1669 (2012).
23. L. Picard *et al.*, DGINN, an automated and highly-flexible pipeline for the detection of genetic innovations on protein-coding genes. *Nucleic Acids Res* **48**, e103 (2020).
24. S. L. Sawyer, L. I. Wu, M. Emerman, H. S. Malik, Positive selection of primate TRIM5alpha identifies a critical species-specific retroviral restriction domain. *Proc Natl Acad Sci U S A* **102**, 2832-2837 (2005).
25. J. W. Bruce, M. Bracken, E. Evans, N. Sherer, P. Ahlquist, ZBTB2 represses HIV-1 transcription and is regulated by HIV-1 Vpr and cellular DNA damage responses. *PLoS Pathog* **17**, e1009364 (2021).
26. F. Forouzanfar *et al.*, HIV-1 Vpr mediates the depletion of the cellular repressor CTIP2 to counteract viral gene silencing. *Sci Rep* **9**, 13154 (2019).
27. T. Kino *et al.*, Human immunodeficiency virus type 1 (HIV-1) accessory protein Vpr induces transcription of the HIV-1 and glucocorticoid-responsive promoters by binding directly to p300/CBP coactivators. *J Virol* **76**, 9724-9734 (2002).
28. B. Romani *et al.*, HIV-1 Vpr reactivates latent HIV-1 provirus by inducing depletion of class I HDACs on chromatin. *Sci Rep* **6**, 31924 (2016).
29. K. Hrecka *et al.*, HIV-1 and HIV-2 exhibit divergent interactions with HLTF and UNG2 DNA repair proteins. *Proc Natl Acad Sci U S A* **113**, E3921-3930 (2016).
30. H. Lahouassa *et al.*, HIV-1 Vpr degrades the HLTF DNA translocase in T cells and macrophages. *Proc Natl Acad Sci U S A* **113**, 5311-5316 (2016).
31. C. H. Douse *et al.*, TASOR is a pseudo-PARP that directs HUSH complex assembly and epigenetic transposon control. *Nat Commun* **11**, 4940 (2020).

32. N. Azzouz, O. O. Panasenko, G. Colau, M. A. Collart, The CCR4-NOT complex physically and functionally interacts with TRAMP and the nuclear exosome. *PLoS One* **4**, e6760 (2009).
33. K. Y. Kong *et al.*, Cotranscriptional recruitment of yeast TRAMP complex to intronic sequences promotes optimal pre-mRNA splicing. *Nucleic Acids Res* **42**, 643-660 (2014).
34. C. Kilchert, S. Wittmann, L. Vasiljeva, The regulation and functions of the nuclear RNA exosome complex. *Nat Rev Mol Cell Biol* **17**, 227-239 (2016).
35. N. Meola *et al.*, Identification of a Nuclear Exosome Decay Pathway for Processed Transcripts. *Mol Cell* **64**, 520-533 (2016).
36. I. Muller *et al.*, MPP8 is essential for sustaining self-renewal of ground-state pluripotent stem cells. *Nat Commun* **12**, 3034 (2021).
37. A. Jordan, D. Bisgrove, E. Verdin, HIV reproducibly establishes a latent infection after acute infection of T cells in vitro. *EMBO J* **22**, 1868-1877 (2003).
38. O. I. Fregoso *et al.*, Evolutionary toggling of Vpx/Vpr specificity results in divergent recognition of the restriction factor SAMHD1. *PLoS Pathog* **9**, e1003496 (2013).
39. D. Schwefel *et al.*, Molecular determinants for recognition of divergent SAMHD1 proteins by the lentiviral accessory protein Vpx. *Cell Host Microbe* **17**, 489-499 (2015).
40. D. Schwefel *et al.*, Structural basis of lentiviral subversion of a cellular protein degradation pathway. *Nature* **505**, 234-238 (2014).
41. N. Laguette *et al.*, Evolutionary and functional analyses of the interaction between the myeloid restriction factor SAMHD1 and the lentiviral Vpx protein. *Cell Host Microbe* **11**, 205-217 (2012).
42. E. S. Lim *et al.*, The ability of primate lentiviruses to degrade the monocyte restriction factor SAMHD1 preceded the birth of the viral accessory protein Vpx. *Cell Host Microbe* **11**, 194-204 (2012).
43. A. Afanasyeva, M. Bockwoldt, C. R. Cooney, I. Heiland, T. I. Gossmann, Human long intrinsically disordered protein regions are frequent targets of positive selection. *Genome Res* **28**, 975-982 (2018).
44. J. Nilsson, M. Grahn, A. P. Wright, Proteome-wide evidence for enhanced positive Darwinian selection within intrinsically disordered regions in proteins. *Genome Biol* **12**, R65 (2011).
45. A. Rosa *et al.*, HIV-1 Nef promotes infection by excluding SERINC5 from virion incorporation. *Nature* **526**, 212-217 (2015).
46. Y. Usami, Y. Wu, H. G. Gottlinger, SERINC3 and SERINC5 restrict HIV-1 infectivity and are counteracted by Nef. *Nature* **526**, 218-223 (2015).
47. S. Jager *et al.*, Vif hijacks CBF-beta to degrade APOBEC3G and promote HIV-1 infection. *Nature* **481**, 371-375 (2011).
48. W. Zhang, J. Du, S. L. Evans, Y. Yu, X. F. Yu, T-cell differentiation factor CBF-beta regulates HIV-1 Vif-mediated evasion of host restriction. *Nature* **481**, 376-379 (2011).
49. S. L. Sawyer, M. Emerman, H. S. Malik, Ancient adaptive evolution of the primate antiviral DNA-editing enzyme APOBEC3G. *PLoS Biol* **2**, E275 (2004).
50. R. Yoshikawa *et al.*, Small ruminant lentiviral Vif proteins commonly utilize cyclophilin A, an evolutionarily and structurally conserved protein, to degrade ovine and caprine APOBEC3 proteins. *Microbiol Immunol* **60**, 427-436 (2016).

51. J. Zhang, D. M. Webb, Rapid evolution of primate antiviral enzyme APOBEC3G. *Hum Mol Genet* **13**, 1785-1791 (2004).
52. P. Lomonte, Herpesvirus Latency: On the Importance of Positioning Oneself. *Adv Anat Embryol Cell Biol* **223**, 95-117 (2017).
53. E. Forte, Z. Zhang, E. B. Thorp, M. Hummel, Cytomegalovirus Latency and Reactivation: An Intricate Interplay With the Host Immune Response. *Front Cell Infect Microbiol* **10**, 130 (2020).
54. L. Riviere *et al.*, HBx relieves chromatin-mediated transcriptional repression of hepatitis B viral cccDNA involving SETDB1 histone methyltransferase. *J Hepatol* **63**, 1093-1102 (2015).
55. V. P. Desai *et al.*, The role of MORC3 in silencing transposable elements in mouse embryonic stem cells. *Epigenetics Chromatin* **14**, 49 (2021).
56. S. Groh *et al.*, Morc3 silences endogenous retroviruses by enabling Daxx-mediated histone H3.3 incorporation. *Nat Commun* **12**, 5996 (2021).
57. M. M. Gaidt *et al.*, Self-guarding of MORC3 enables virulence factor-triggered immunity. *Nature* **600**, 138-142 (2021).
58. E. Sloan, A. Orr, R. D. Everett, MORC3, a Component of PML Nuclear Bodies, Has a Role in Restricting Herpes Simplex Virus 1 and Human Cytomegalovirus. *J Virol* **90**, 8621-8633 (2016).
59. K. Fukuda, A. Okuda, K. Yusa, Y. Shinkai, A CRISPR knockout screen identifies SETDB1-target retroelement silencing factors in embryonic stem cells. *Genome Res* **28**, 846-858 (2018).
60. N. Liu *et al.*, Selective silencing of euchromatic L1s revealed by genome-wide screens for L1 regulators. *Nature* **11**, 7687
(2018).
61. L. Robbez-Masson *et al.*, The HUSH complex cooperates with TRIM28 to repress young retrotransposons and new genes. *Genome Res* **28**, 836-845 (2018).
62. A. Molaro, H. S. Malik, Hide and seek: how chromatin-based pathways silence retroelements in the mammalian germline. *Curr Opin Genet Dev* **37**, 51-58 (2016).
63. V. M. Jovanovic *et al.*, Positive Selection in Gene Regulatory Factors Suggests Adaptive Pleiotropic Changes During Human Evolution. *Front Genet* **12**, 662239 (2021).
64. T. Wang *et al.*, Epigenetic restriction of Hippo signaling by MORC2 underlies stemness of hepatocellular carcinoma cells. *Cell Death Differ* **25**, 2086-2100 (2018).
65. Y. Xue *et al.*, Arabidopsis MORC proteins function in the efficient establishment of RNA directed DNA methylation. *Nat Commun* **12**, 4292 (2021).
66. M. Seczynska, S. Bloor, S. M. Cuesta, P. J. Lehner, Genome surveillance by HUSH-mediated silencing of intronless mobile elements. *Nature* 10.1038/s41586-021-04228-1 (2021).
67. A. Koch *et al.*, MORC Proteins: Novel Players in Plant and Animal Health. *Front Plant Sci* **8**, 1720 (2017).
68. A. Losada, T. Hirano, Dynamic molecular linkers of the genome: the first decade of SMC proteins. *Genes Dev* **19**, 1269-1287 (2005).
69. L. Dupont *et al.*, The SMC5/6 complex compacts and silences unintegrated HIV-1 DNA and is antagonized by Vpr. *Cell Host Microbe* 10.1016/j.chom.2021.03.001 (2021).
70. I. D. Irwan, H. P. Bogerd, B. R. Cullen, Epigenetic silencing by the SMC5/6 complex mediates HIV-1 latency. *Nat Microbiol* 10.1038/s41564-022-01264-z (2022).

71. A. Decorsiere *et al.*, Hepatitis B virus X protein identifies the Smc5/6 complex as a host restriction factor. *Nature* **531**, 386-389 (2016).
72. C. M. Murphy *et al.*, Hepatitis B Virus X Protein Promotes Degradation of SMC5/6 to Enhance HBV Replication. *Cell Rep* **16**, 2846-2854 (2016).
73. F. Abdul *et al.*, Smc5/6 Antagonism by HBx Is an Evolutionarily Conserved Function of Hepatitis B Virus Infection in Mammals. *J Virol* **92** (2018).
74. R. C. Edgar, MUSCLE: multiple sequence alignment with high accuracy and high throughput. *Nucleic Acids Res* **32**, 1792-1797 (2004).
75. S. Guindon *et al.*, New algorithms and methods to estimate maximum-likelihood phylogenies: assessing the performance of PhyML 3.0. *Syst Biol* **59**, 307-321 (2010).
76. S. L. Pond, S. D. Frost, S. V. Muse, HyPhy: hypothesis testing using phylogenies. *Bioinformatics* **21**, 676-679 (2005).
77. Z. Yang, PAML 4: phylogenetic analysis by maximum likelihood. *Mol Biol Evol* **24**, 1586-1591 (2007).
78. L. Gueguen *et al.*, Bio++: efficient extensible libraries and tools for computational molecular evolution. *Mol Biol Evol* **30**, 1745-1750 (2013).
79. J. Jumper *et al.*, Highly accurate protein structure prediction with AlphaFold. *Nature* **596**, 583-589 (2021).
80. T. Gramberg, N. Sunseri, N. R. Landau, Evidence for an activation domain at the amino terminus of simian immunodeficiency virus Vpx. *J Virol* **84**, 1387-1396 (2010).
81. C. Goujon *et al.*, With a little help from a friend: increasing HIV transduction of monocyte-derived dendritic cells with virion-like particles of SIV(MAC). *Gene Ther* **13**, 991-994 (2006).
82. F. Ueno *et al.*, Vpx and Vpr proteins of HIV-2 up-regulate the viral infectivity by a distinct mechanism in lymphocytic cells. *Microbes Infect* **5**, 387-395 (2003).
83. M. Nomaguchi, N. Doi, A. Adachi, Virological characterization of HIV-2 vpx gene mutants in various cell systems. *Microbes Infect* **16**, 695-701 (2014).
84. I. du Chene *et al.*, Suv39H1 and HP1gamma are responsible for chromatin-mediated HIV-1 transcriptional silencing and post-integration latency. *EMBO J* **26**, 424-435 (2007).
85. T. C. Roberts *et al.*, Quantification of nascent transcription by bromouridine immunocapture nuclear run-on RT-qPCR. *Nat Protoc* **10**, 1198-1211 (2015).

A.

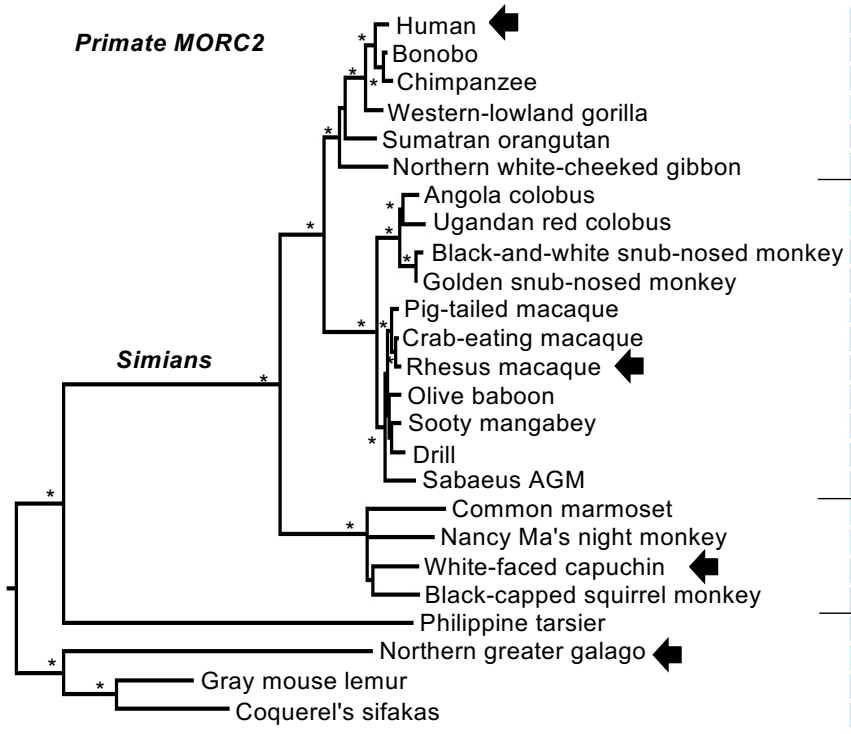

D.

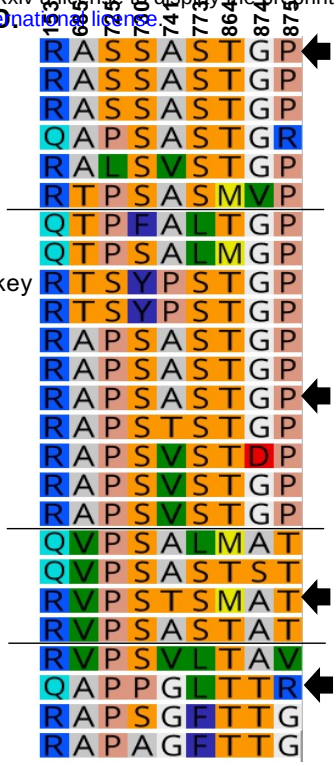

B.

Gene	Dataset (n species)	Positive selection analyses: BUSTED (p value)	PAML CodeML M1 vs M2 (p value)	PAML CodeML M7 vs M8 (p value)	Bio++ M1 vs M2 (p value)	Bio++ M7 vs M8 (p value)
MORC2	Primates (25)	**Yes (0.02)**	**Yes (0.000002)**	**Yes (0.001)**	No (0.71)	**Yes (8.56 E-06)**
	Simians (21)	No (0.19)	**Yes (0.000006)**	**Yes (0.00003)**	**Yes (0.18)**	**Yes (9.66 E-07)**

C.

Gene	Dataset (n species)	Length (codons)	Sites under PS	MEME (p<0.1)	FUBAR (PP>0.9)	PAML M2 (BEB PP>0.9)	PAML M8 (BEB PP>0.95)	Bio++ M8 (PP>0.95)
MORC2	Primates (25)	1032	6	**153**, 625, 653, 725, **730**, **741**, 772, **875**, 879	**153**, **730**, **875**	**741**, **773**, **874**, **875**	**153**, 706, **730**, **741**, **773**, **874**, **875**	**153**, **741**, **773**, **874**, **875**
	Simians (21)	1032	7	**153**, 625, 653, **685**, **725**, **741**, 772, **874**, 879	**153**, **685**, **725**, **874**	**153**, **685**, **725**, **741**, **773**, **864**, **874**	**153**, **685**, **725**, **741**, **773**, **864**, **874**	**153**, **685**, **725**, **741**, **773**, **864**, 873, **874**

E.

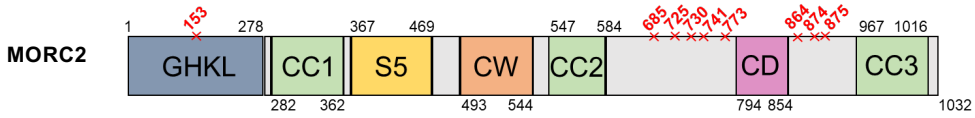

F.

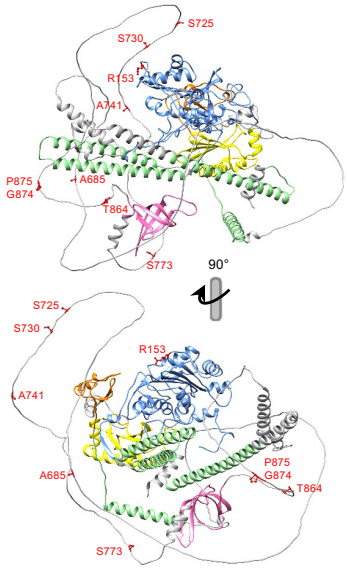

G.

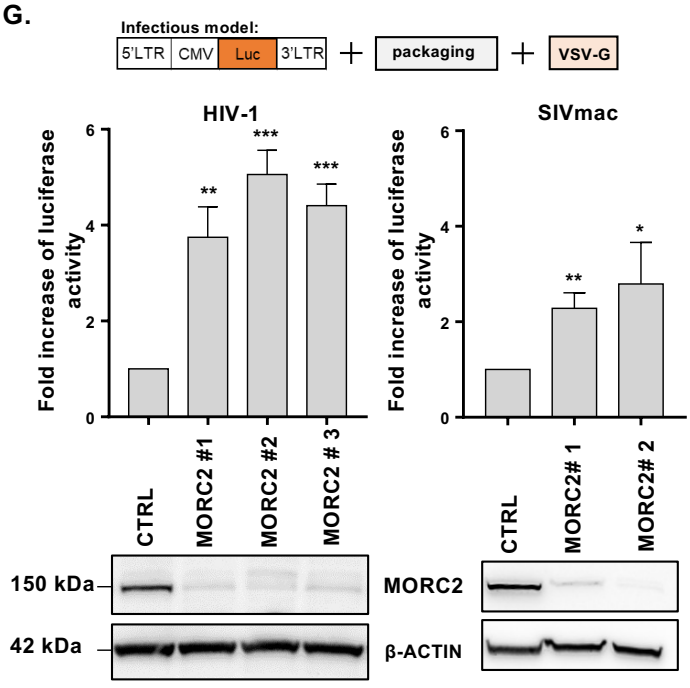

H.

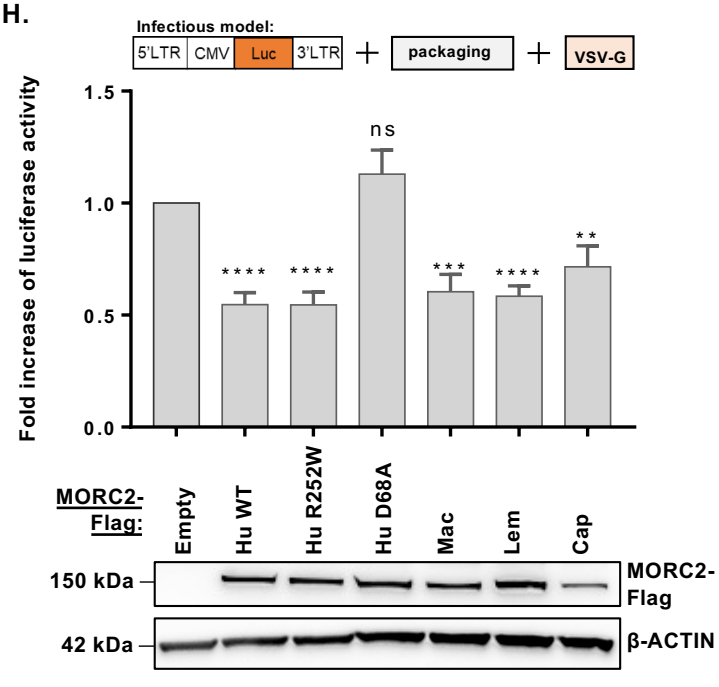

Figure 1

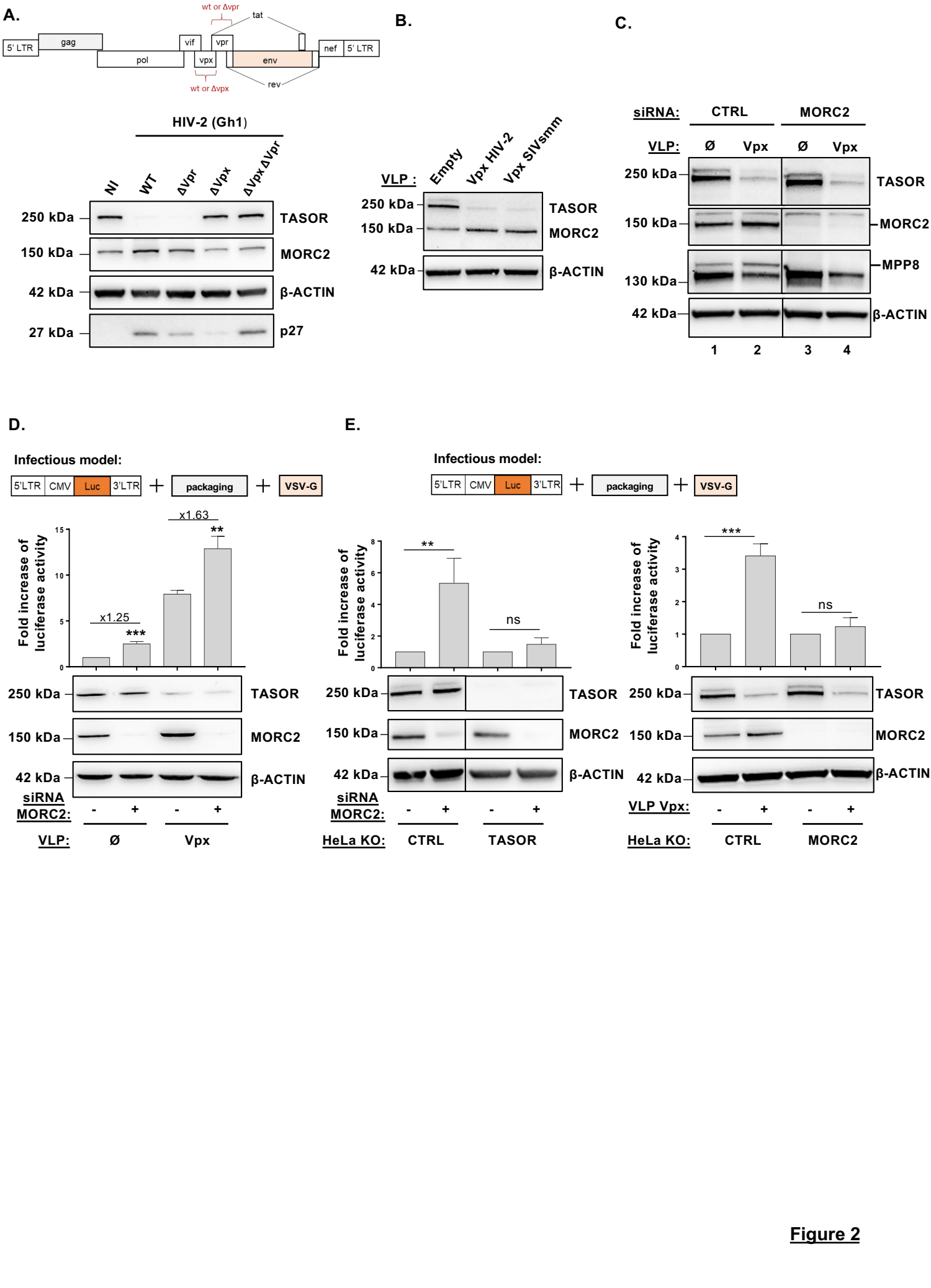

Figure 2

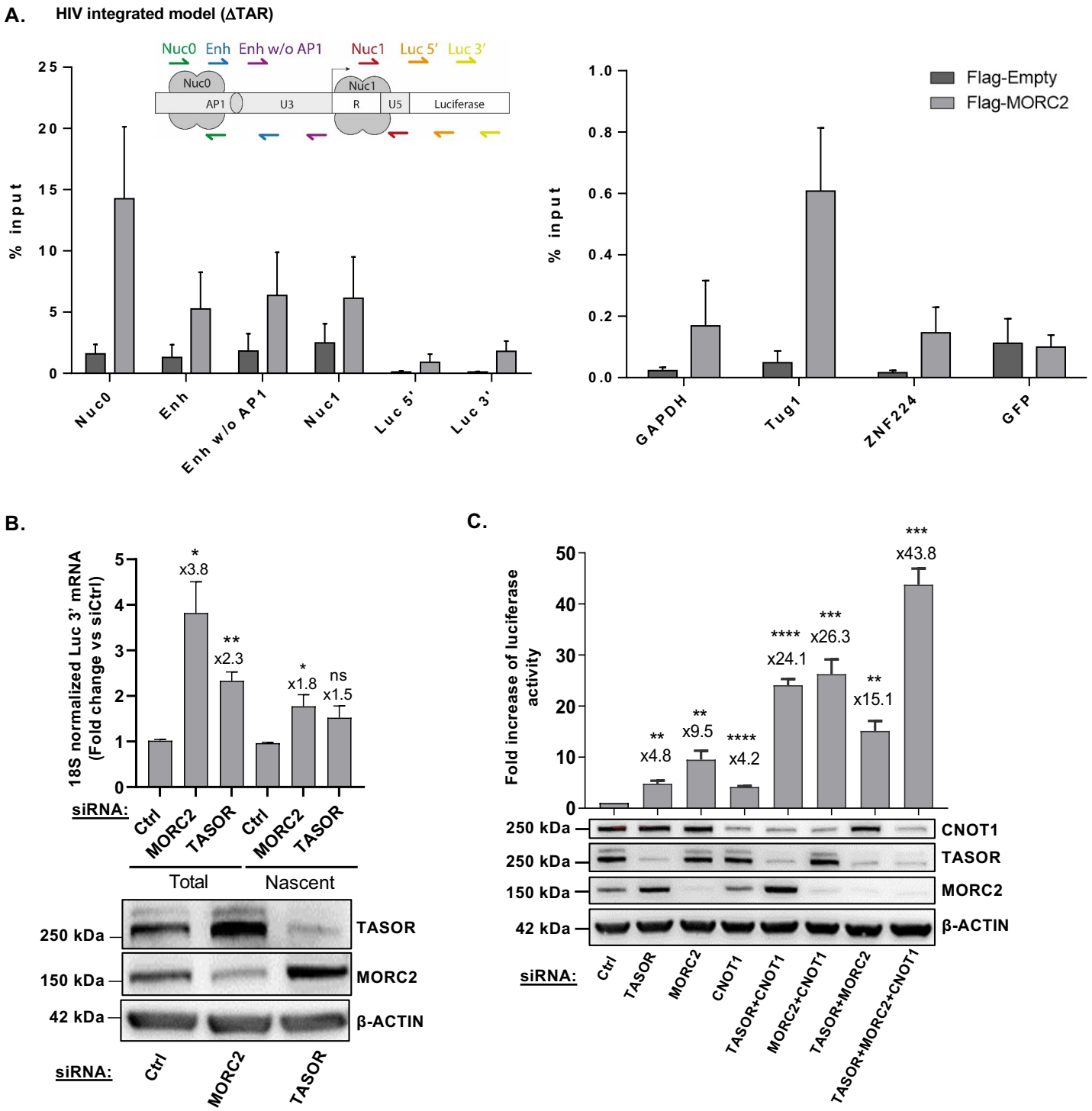

Figure 3

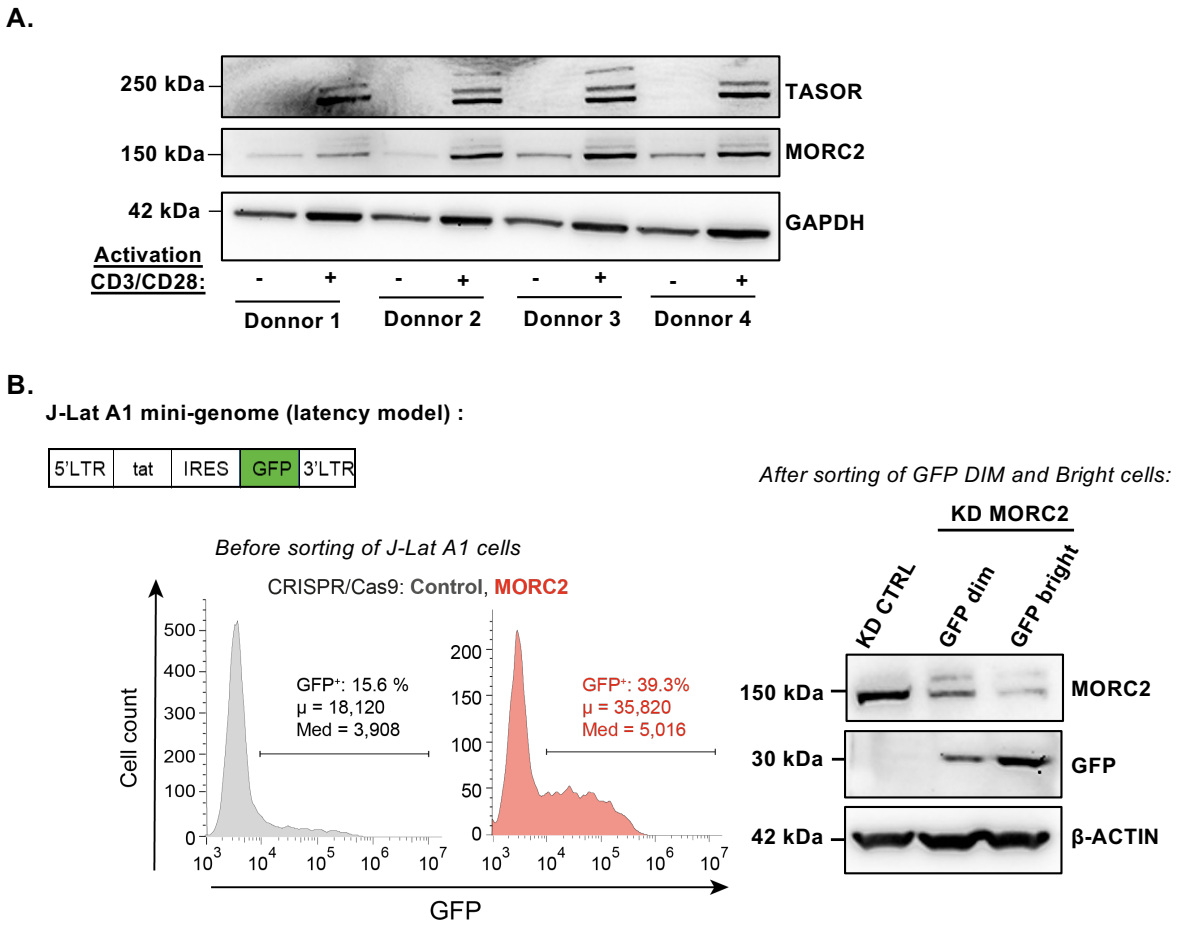

Figure 4

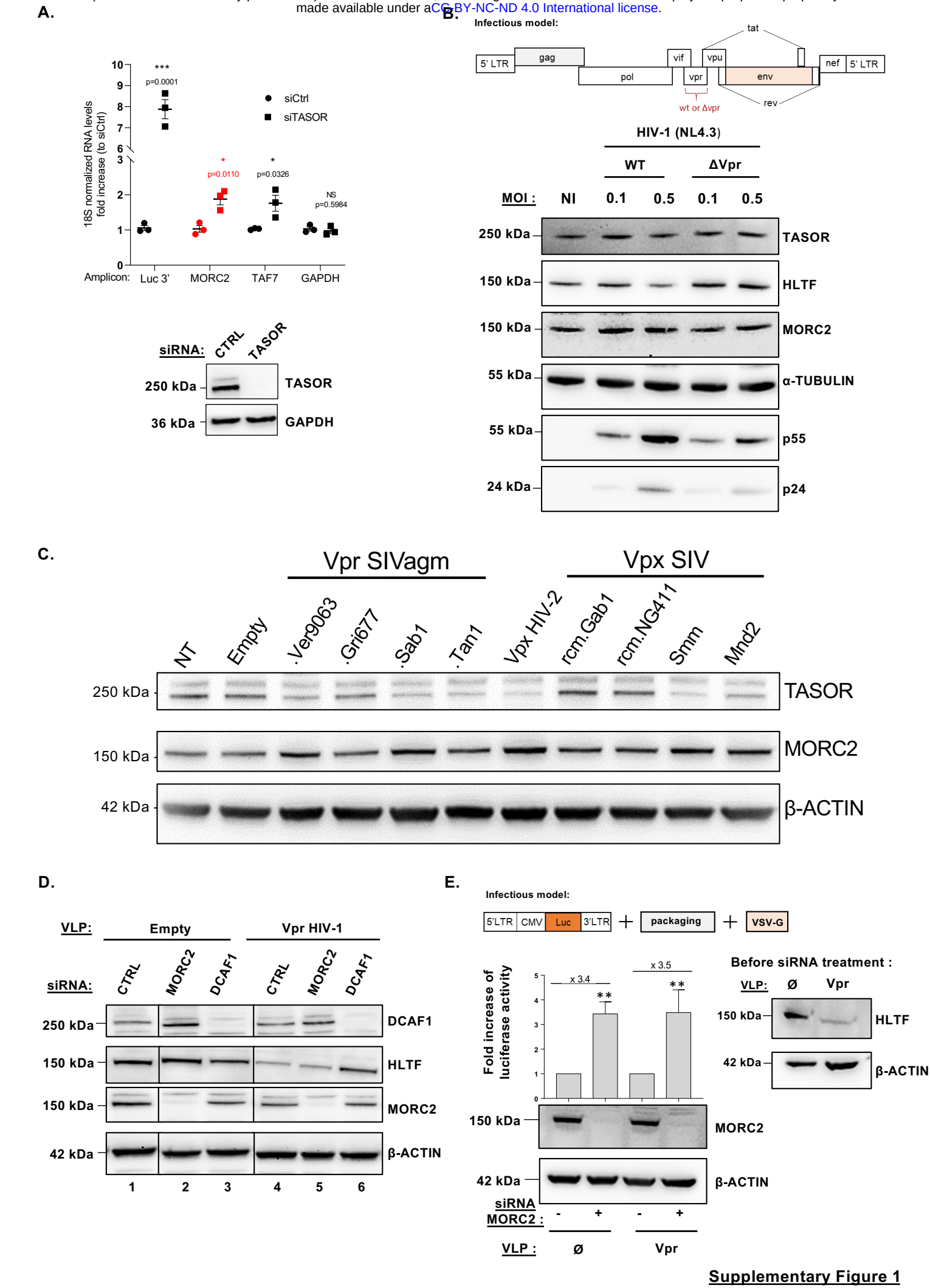

Supplementary Figure 1

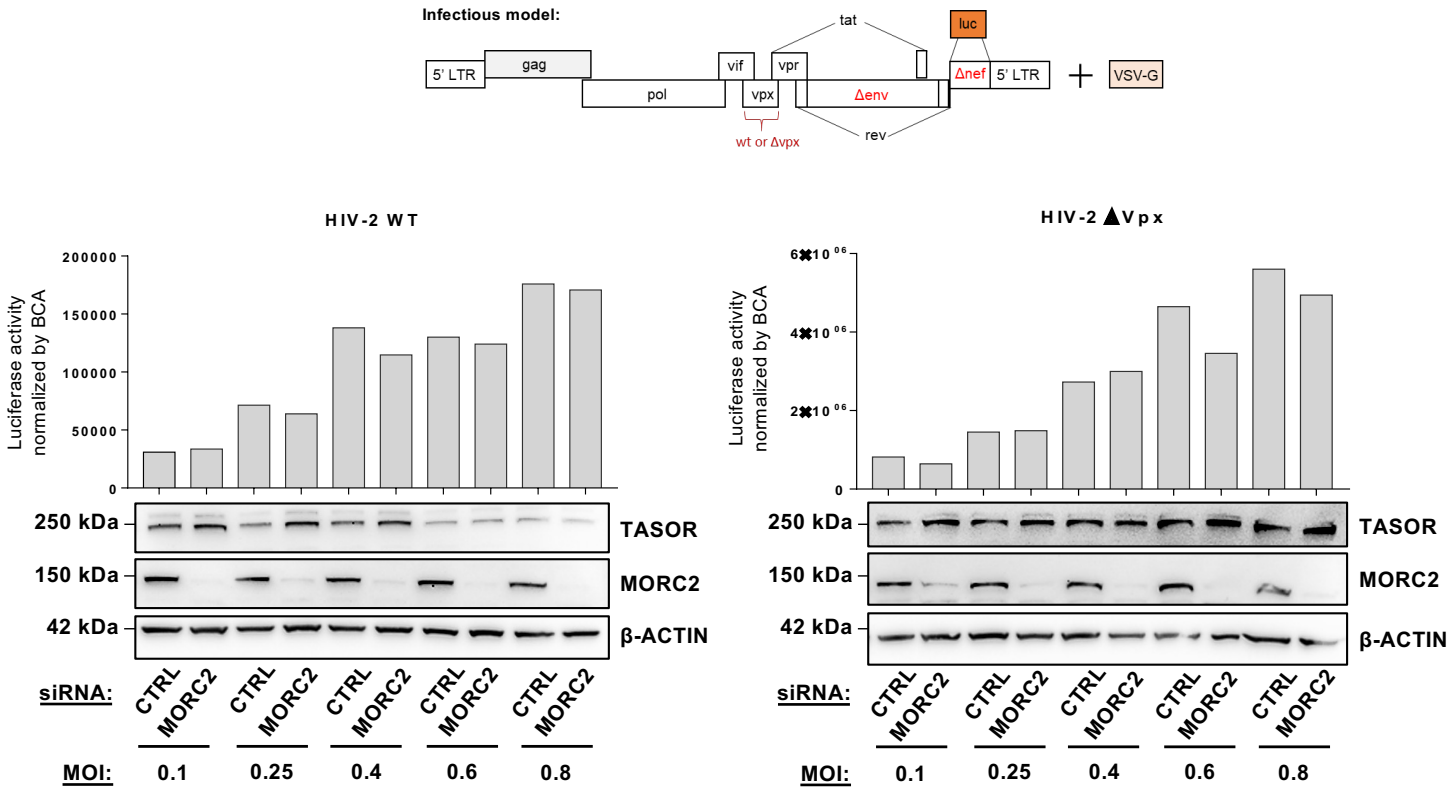

Supplementary Figure 2

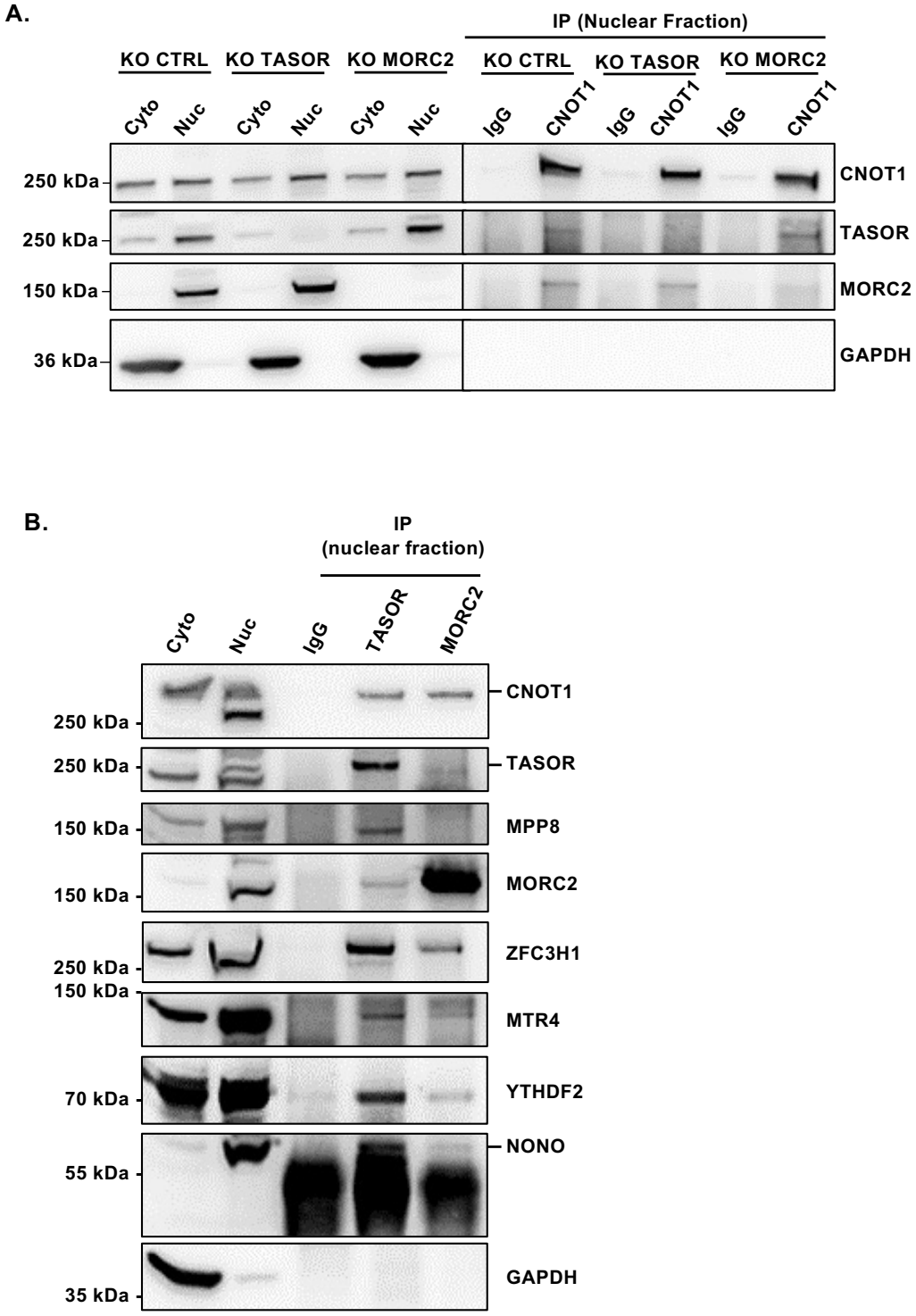

Supplementary Figure 3

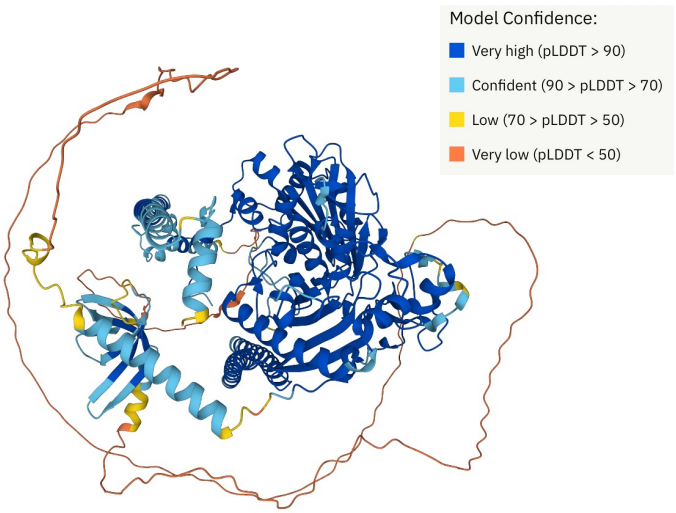

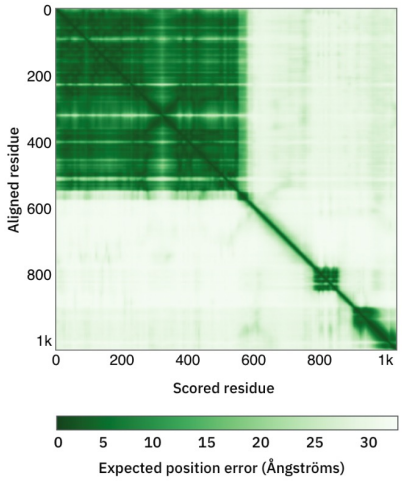

Supplementary Figure 4